




Crip2 affects vascular development by fine-tuning endothelial cell aggregation and proliferation

Shuaiqi Yang¹ · Xiangmin Zhang¹ · Xianpeng Li³ · Hongyan Li^{1,2,4} 

Received: 6 January 2025 / Revised: 4 February 2025 / Accepted: 14 February 2025
© The Author(s) 2025

Abstract

Endothelial cell adhesion and migration are crucial to various biological processes, including vascular development. The identification of factors that modulate vascular development through these cell functions has emerged as a prominent focus in cardiovascular research. Crip2 is known to play a crucial role in cardiac development, yet its involvement in vascular development and the underlying mechanism remains elusive. In this study, we revealed that Crip2 is expressed predominantly in the vascular system, particularly in the posterior cardinal vein and caudal vein plexus intersegmental vein. Upon Crip2 loss, the posterior cardinal vein plexus and caudal vein plexus are hypoplastic, and endothelial cells exhibit aberrant aggregation. In human umbilical vein endothelial cells (HUVECs), CRIP2 interacts with the cytoskeleton proteins KRT8 and VIM. The absence of CRIP2 negatively regulates their expression, thereby fine-tuning cytoskeleton formation, resulting in a hyperadhesive phenotype. Moreover, CRIP2 deficiency perturbs the VEGFA/CDC42 signaling pathway, which in turn diminishes the migrating capacity of HUVECs. Furthermore, the loss of CRIP2 impairs cell proliferation by affecting its interaction with SRF through PDE10A/cAMP and PDGF/JAK/STAT/SRF signaling. Collectively, our findings delineate a crucial role for CRIP2 in controlling the migration, adhesion and proliferation of endothelial cells, thereby contributing to vascular development in zebrafish. These insights may provide a deeper understanding of the etiology of cardiovascular disorders.

Keywords Crip2 · Vascular development · Cell aggregation · Cell proliferation

Introduction

The cardiovascular system, the most vital system of vertebrates, transports oxygen, nutrients and signaling factors to all body cells and removes waste. A healthy, complete cardiovascular system is indispensable for normal

physiological function. Vascular abnormalities frequently contribute to circulatory system diseases, such as aneurysms [1], arteriovenous malformations [2], venous malformations [3], and arteriovenous fistulas [4], which largely stem from endothelial cell dysfunction. For example, arteriovenous fistula (AVF) primarily results from abnormal connections between veins and arteries due to embryonic intimal hyperplasia, which is caused mainly by endothelial dysfunction, abnormal cell proliferation and migration [4–6].

Normal vascular development, including vasculogenesis and angiogenesis, is crucial for the survival and growth of organisms. Vasculogenesis involves endothelial progenitor cells from the embryonic mesoderm gradually forming a primitive vascular plexus and blood cells through fate determination, cell proliferation and differentiation [7]. Angiogenesis, on the other hand, involves the formation of a functionally intact circulatory system by sprouting from preexisting blood vessels, incorporating processes such as vessel destabilization, angiogenic signals, tip and stalk cell selection, guidance, lumen formation, and vessel maturation

✉ Hongyan Li
hongyanli@ouc.edu.cn

¹ College of Marine Life Sciences, Key Laboratory of Evolution & Marine Biodiversity (Ministry of Education), Institute of Evolution & Marine Biodiversity, Ocean University of China, Qingdao 266003, China

² Laboratory for Marine Biology and Biotechnology, Qingdao Marine Science and Technology Center, Qingdao, China

³ Institute of Brain Science and Brain-inspired Research, Shandong First Medical University & Shandong Academy of Medical Sciences, Jinan, China

⁴ Ocean University of China, Room 301, Darwin Building, 5 Yushan Road, Qingdao 266003, China

[8]. This requires coordinated endothelial cell activities, including proliferation, differentiation, migration, adhesion, and cell-cell interactions, which are regulated by signaling pathways such as the Wnt/Frizzled, Delta/Notch, Ephrin/Eph, TGF, PDGF, and VEGF pathways, as well as transcription factors such as TAL1, RUNX-1 and ETS [9–14]. For example, VEGF signaling plays a role in regulating angiogenesis and disease and is correlated with invasiveness, vascular density, metastasis, recurrence and proliferation [15]. PDGF has been demonstrated to be a proangiogenic factor, and the PDGF/PDGFR signaling pathway is considered an important receptor tyrosine kinase (RTK) pathway that promotes the proliferation, invasion, metastasis, and angiogenesis of tumor cells [16]. Investigating the factors influencing these activities is crucial for understanding endothelial cell physiology.

To establish a normal vascular structure and regulate various physiological responses, endothelial cells work together with smooth muscle cells and fibrocytes to create a highly organized structure referred to as the ‘mini-lumen structure’. This intricate network of cell-cell interactions is primarily established by the cell aggregation process, which relies on a multitude of cell-cell adhesion proteins, prominent among which are those belonging to the cadherin superfamily [17]. Disruption of cell aggregation can arise from various factors, including the loss of functional E-cadherin, varied adhesion to the extracellular matrix, or a response to inflammatory cytokines [18–20]. The adhesion of cells is frequently regulated by their interactions with the cell-extracellular matrix (ECM) and integrin signaling; this activation initiates a cascade of biological processes, such as cytoskeleton dynamics, cell motility, and cell maturation [21, 22]. Alterations in the adhesive capacity of tumor cells can lead to cancer metastasis; for example, the loss of E-cadherin function is associated with a more invasive phenotype [23, 24]. Proper cell aggregation, driven by effective cell adhesion and migration, is therefore critical for angiogenesis.

Eukaryotic cells rely on the cytoskeleton to establish a systemic architecture that serves diverse functions. The cytoskeleton not only provides stress points for mechanical forces that facilitate cell movement but also offers anchors and stress points for cell junctions. Moreover, it plays a crucial role in a variety of complex cellular phenomena, including cell division, migration, adhesion, junctions, endocytosis, intracellular transport, force transmission and responses to stress [25–29]. The eukaryotic cytoskeleton is composed of actin filaments, intermediate filaments, and microtubules, and the dynamics of this structure are driven by motor proteins such as myosin, kinesin, and dynein, which are responsible for polymerization and intracellular transport [30]. Intermediate filaments, in particular, are

integral to several cellular processes, including apoptosis, cell junctions, migration, adhesion, and interactions with other cytoskeletal components [31]. Understanding how the cytoskeleton, specifically cell adhesion, migration and invasion, affects cardiovascular diseases and tumor angiogenesis is highly important. This knowledge can provide critical insights into the mechanisms underlying these complex pathologies.

LIM proteins, characterized by the presence of classical LIM (Lin-11, Isl1, MEC-3) domains, act as adapters or scaffolds that facilitate the assembly of multimeric protein complexes [32, 33]. In mammals, these proteins are pivotal in regulating a diverse array of biological processes, including signal transduction regulation, cell proliferation, migration, junction formation, adhesion and cytoskeletal organization [34–37]. Research has revealed that 41 LIM proteins are enriched in cell junctions and the actomyosin cytoskeleton [38, 39]. Among these proteins, 26 (including CSRP, ZYXIN, PAXILLIN, and LIMD1) have been identified to be involved in cell adhesion and junction processes, 21 of which respond to myosin II activity [40]. CRIP (cysteine-rich intestinal protein) proteins, including Crip1 and Crip2, constitute one subgroup of LIM proteins. Crip1 regulates cell proliferation, migration, and invasion, as well as epithelial-mesenchymal transition [41–43]. Crip2 is known to be involved in cardiac development [44–46], but its involvement in the formation of blood vessels remains elusive.

In this study, we explored the role of Crip2 in zebrafish vascular development and elucidated the underlying mechanism via human vascular endothelial cells. Our findings demonstrate that Crip2 is crucial for zebrafish vascular development. Crip2 interacts with the transcription factor SRF and the cytoskeleton proteins Krt8 and Vim, through these interactions, it orchestrates the regulation of both its function and downstream factors. This regulation is pivotal in controlling the migration, adhesion and proliferation of endothelial cells, thereby participating in vascular development in zebrafish. These insights contribute to a better understanding of the etiology of cardiovascular disorders.

Materials and methods

Zebrafish maintenance, transgene generation and knockout line generation

The AB strain of zebrafish (*Danio rerio*) was maintained in a standard zebrafish culture system (Haisheng Zebrafish Circulation Culture Tank, Shanghai, China) at 28.5 °C and fed twice daily under a 14-h light/10-h dark cycle. After zebrafish naturally mated, fertilized embryos were collected and cultured in an E3 medium.

The transgene zebrafish were produced with a Tol2 kit [47]. Briefly, the *crip2* promoter sequence (-8000 ~ -1 bp) and CDS were amplified with PrimeSTAR GXL DNA Polymerase (Takara, R050A), subcloned and inserted into p5E-MCS and pME-MCS, respectively. The two plasmids and p3E-polyA were recombined into pDestTol2pA2 with LR Clonase (Invitrogen, 12538120), and the transposase mRNA was synthesized with a T7 mRNA Kit (Invitrogen, AM1344). Then, the transgenic recombinant plasmid and transposase mRNA were mixed to obtain a 100 ng/ μ L mRNA and 50 ng/ μ L plasmid mixture. Then, 1 nL of mixed solution was injected into 1-cell-stage embryos in either the yolk or the cell cytoplasm via microinjection. The transgenic F0 founder embryos or produced F1 embryos were screened by examination of tissue-specific green fluorescence.

CRISPR/Cas9 was used to generate the *crip2* knockout zebrafish strain. The appropriate target site (Supplemental information - Primer) on the exon within the first third of the CDS was designed via CRISPOR (<http://crispor.tefor.net/>). The forward primer, which contains a T7 promoter and guide sequence, and the reverse primer, which encodes the standard chimeric sgRNA scaffold, were used with the sgRNA scaffold plasmid to generate the templates for sgRNA production. The sgRNA was transcribed in vitro with purified templates and T7 RNA Polymerase (Yeasen, 36705ES48). The Cas9 protein (NEB, M0646M) was mixed 1:1 with the sgRNA for a 2 μ M Cas9, 0.5 μ g/ μ L sgRNA solution to generate Cas9 RNP complexes. Then, 1 nL of Cas9 RNP complexes was injected into 1-cell-stage embryos via microinjection. The injected F0 adult zebrafish were mated with wild-type zebrafish to produce F1 embryos. The mutation types of F1 adult zebrafish were identified by T7 endonuclease I identification and Sanger sequencing. F2 embryos were produced by mating F1 adults with the same mutation type.

Whole-mount in situ hybridization and quantitative real-time PCR

For whole-mount in situ hybridization (WISH), the embryos were maintained in E3 medium supplemented with 0.0045% 1-phenyl-2-thiourea (PTU; Sigma, 189235), which prevented pigmentation 24 h post-fertilization (hpf). The embryos were sorted and fixed with 4% paraformaldehyde (PFA; Sigma, 158127) following the instructions of Kimmel [48]. Fragments of *crip2* and other markers were amplified via PCR using the specific primers (Supplemental information - Primer) designed via Primer Premier 6.0 on the basis of the NCBI database. The purified fragments were subcloned and inserted into the pEASY-T3 vector (TransGen, CT301), and the vectors were subsequently sequenced successfully and digested into linearized plasmids by a specific

restriction enzyme. The antisense riboprobes labeled with digoxigenin-11-UTP (Roche, 11277073910) were synthesized via in vitro transcription with Sp6 RNA polymerase (Invitrogen, EP0131) or T7 RNA polymerase (Promega, P2075). The WISH experimental procedures followed the standard protocol [49]. After staining, the embryos were mounted in glycerin, and photographed under a stereomicroscope (Nikon, Japan).

RNA was extracted from multiple tissues of zebrafish, and the cDNAs were reverse transcribed following a previous standard protocol [50]. Quantitative real-time PCR (qRT-PCR) was conducted via SYBR qPCR Master Mix (Vazyme, Q431) on an ABI 7500 real-time PCR system (Applied Biosystems, Singapore). The figures showing the relative expression levels of each gene were generated with GraphPad Prism 9.

Cell culture and subcellular localization

Human umbilical vein endothelial cells (HUVECs) were cultured in RPMI 1640 medium (VivaCell, C3010) containing 10% fetal bovine serum (FBS; Yeasen, 40130ES76) and 1% penicillin-streptomycin solution (Cytiva, SV30010) in a 37 °C humidified incubator with 5% CO₂. HEK293T cells were maintained in high-glucose DMEM (VivaCell, C3113) supplemented with 10% FBS and 1% penicillin-streptomycin solution. Cell transfections were carried out via Liposomal Transfection Reagent (Yeasen, 40802ES03) following the manufacturer's instructions.

The *pcDNA3.1/V5/eGFP* vector was formed by cloning the *eGFP* gene into the eukaryotic expression vector *pcDNA3.1/V5-His A*. The purified *crip2* coding sequence was subsequently subcloned and inserted into the linearized *pcDNA3.1/V5/eGFP* vector via homologous recombination with using ClonExpress Mix (Vazyme, C115) [51]. The recombinant plasmid and *pcDNA3.1/V5/eGFP* were individually transfected into HEK293T cells. Twenty-four hours after transfection, DAPI was used to stain the cell nucleus. After being washed with PBS, the samples were observed and photographed under a confocal microscope (Leica, SP8).

Lentivirus and cell line generation

The human *CRIP2* knockout target sites (Supplemental information- Primer) that were designed as above and the *CRIP2* CDS that carried a Flag sequence tag, were fused into the linearized lentiCRISPR v2 and pLVX-mCMV-ZsGreen1-Puro, respectively. As negative controls in the knockout assays, the target sites of the nonessential and noncoding human *Rosa26* locus were also subcloned [52]. HEK293T cells were cotransfected with the above lentiviral

vectors (negative controls, recombinant lentiCRISPR v2 and pLVX-mCMV-ZsGreen1-Puro) and packaging vectors (pMD2G, Addgene, 12259; psPAX2, Addgene, 12260). Lentiviruses were collected and concentrated via a Lentivirus Concentration Solution Kit (Yeasen, 41101ES50). After transfection into HUVECs, 4 µg/ml puromycin (Solarbio, P8230) was used to select stable cells, and the monoclonal knockout cells were screened and grown in 48-well plates. The surviving cells were expanded and confirmed by western blotting.

Immunofluorescence, EdU and TUNEL assays

HUVECs were cultured in 12-well plates for 18 h. The cells, fixed with 4% PFA and incubated with 0.5% Triton X-100, were stained with specific antibodies at their specified optimal dilutions overnight at 4 °C. They were stained with Alexa Fluor 488 (Invitrogen, A21121) or Alexa Fluor Plus 488 (Invitrogen, A48282TR) for 1 h at room temperature, followed by nuclear staining with DAPI. If needed, TRITC phalloidin (Yeasen, 40734ES75) was used to stain F-actin at a final dilution of 1:200. The cells were observed and imaged under a confocal microscope.

The proliferation of the cells was determined via an EdU Cell Proliferation Kit (Invitrogen, C10337) according to the manufacturer's instructions. Briefly, HUVECs were cultured in 24-well plates for 12 h and then labeled with 10 µM EdU for 2 h. The cells were washed with PBS, fixed in 4% PFA, incubated with 0.5% Triton X-100, stained with DAPI and imaged under a confocal microscope. The percentages of EdU⁺ cells among all the DAPI⁺ cells were determined.

The detection and quantification of apoptotic cell death were performed via an In Situ Cell Death Detection Kit (Roche, 12156792910) according to the manufacturer's instructions. As a negative control, the TUNEL reaction mixture without Enzyme Solution was used to stain the HUVECs. As positive controls, the cells were treated with DNase I for 10 min before staining. Other experimental treatments were performed as described above.

Transwell and adhesion assays

The effect of *CRIP2* deficiency on the migration and invasion of HUVECs was determined with transwell migration and invasion assays [53]. HUVECs were seeded into 6-well plates and grown until they reached confluence. After starvation for 12 h in a medium without FBS, a surrogate scratch "wound" was produced on each confluent monolayer of cells via a 200 µL sterile pipette tip. At 0, 12, 24, 36, and 48 h after wounding, the scratch area was recorded and photographed under an inverted fluorescence microscope (Leica, DMI3000 B). The degree of wound closure

was investigated via ImageJ, and the results were plotted as the repair rate of the scratch of cells via the following formula: [(scratch area at time zero – scratch area after individual treatment period) ÷ (scratch area at time zero)] × 100%.

The cells were precoated with fibronectin solution (Sigma, F0556) for 1 h in 12-well plates at 37 °C. HUVECs were seeded and cultured in a humidified incubator for 0.5, 1, 2 h. The cells were fixed in 4% PFA, stained with crystal violet ammonium oxalate solution (Solarbio, G1062), and imaged under a confocal microscope. The adherent cells were counted via ImageJ.

Immunoprecipitation, coimmunoprecipitation and Western blotting

HUVECs, expressing the CRIP2-Flag fusion protein, were lysed in cold cell lysis buffer containing protease and phosphatase inhibitors (Beyotime, P1045). Centrifugation was performed to remove cell debris. The cell lysates were then incubated with anti-Flag (BioLegend, 637319) or control isotype IgG with gentle agitation at 4 °C overnight. The immunocomplexes were subsequently precipitated with protein A/G magnetic beads (MCE, HY-K0202) at 4 °C for 4 h. The magnetic beads were washed with PBST and heated with protein sample loading buffer at 100 °C for 5 min. The protein electrophoresis of the samples was performed via PAGE (Epizyme, PG113), after which the gels were stained with Coomassie Brilliant blue R250 (Sigma, 1.12553). The particular protein bands were removed for mass spectrometry (done by Sangon, China).

The human *CRIP2* and *KRT8*, *SRF*, and *VIM* CDSs were amplified and inserted into *pCMV-C-Flag* and *pCMV-C-HA*, respectively. HEK293T cells were transfected with the recombinant plasmids together. Twenty-four hours after transfection, the cells were collected and lysed to obtain the cell lysates. Other experimental treatments were performed as described above to obtain protein samples. The protein samples were analyzed via western blotting.

The cells were lysed with cell lysis buffer containing protease and phosphatase inhibitors at 4 °C for 30 min and detached from the culture plates. The lysates were subsequently centrifuged at 12,000 × g at 4 °C for 15 min. The protein concentration was detected via a BCA protein assay kit (CWBIO, CW0014) [54], and the samples were subsequently heated with a protein sample loading buffer at 100 °C for 5 min. Equal amounts of the protein samples were electrophoresed via 12.5% PAGE. The proteins were transferred to polyvinylidene fluoride (PVDF; Millipore, IPVH00010) membranes. The PVDF membranes were blocked with 5% BSA in PBST for 3 h at room temperature, incubated with a specific antibody (Supplemental information- Antibody) at 4 °C overnight, and then with

a horseradish peroxidase-conjugated goat anti-rabbit (or mouse) IgG antibody at room temperature for 1 h. Anti-GAPDH (1:1000; Proteintech, 60004-1-Ig) was used for internal standardization. The membranes were subsequently observed and photographed using a Mini Chemi fluorescence imaging analysis system. The band intensity was analyzed via ImageJ software.

Statistical analysis

In this study, data acquisition from the figures was achieved predominantly via ImageJ software. Subsequent data analysis and the generation of charts were performed with GraphPad Prism 9 software. All the results are presented as the means \pm SDs from three independent experiments. A P -value < 0.05 was considered statistically significant. Data across different groups were analyzed via unpaired t -test, or one-way ANOVA or two-way ANOVA, as appropriate.

Data retrieval

The transcript sequences and protein sequences of all the species included in the present study were searched for and downloaded from the NCBI database. Figure S1 illustrates the expression of Crip2 in zebrafish obtained from the Atlas for Zebrafish Development provided by the UCSC Cell Browser (<http://cells.ucsc.edu/?ds=zebrafish-dev>) and Daniocell (<https://daniocell.nichd.nih.gov>). Additionally, Fig. S8, which presents the predicted interacting proteins of human CRIP2, was generated from data retrieved from STRING (<https://cn.string-db.org/>).

Results

crip2 is persistently expressed in the cardiovascular system

Previous studies have reported the expression profiles of *crip2* in zebrafish early embryos up to 48 hpf [44, 45]. In this study, we presented a detailed examination of *crip2* expression patterns at various stages prior to 120 hpf via WISH. From the 2-cell stage to the 6 hpf stage, *crip2* was ubiquitously expressed in the animal pole of the embryo, and its expression level gradually decreased with development (Fig. 1A–D), indicating that it was maternally expressed. The expression of *crip2* begins in the notochord at 10 hpf, increases by 14 hpf and ceases at 48 hpf (Fig. 1E–I). The expression of *crip2* was also visible in the myotome between 18 hpf and 48 hpf (Fig. 1G–I). From 18 hpf onward, *crip2* transcripts were predominantly found in the embryonic blood vascular system, including the heart and eye

blood vessel endothelial cells at 18 hpf (Fig. 1G), as well as the caudal vein plexus at 24 hpf (Fig. 1H). By 48 hpf, the expression was observed in the intersegmental vein and posterior cardinal vein (Fig. 1I), with this pattern persisting up to 120 hpf (Fig. 1J–L). In addition, *crip2* was detected in the pharyngeal arch (Fig. 1I) and outer nuclear layer (Fig. 1K, L). These findings indicate that *crip2* exhibits a dual pattern of maternal expression followed by tissue-specific but dynamic expression during early zebrafish embryonic development. Furthermore, *crip2* is continuously expressed in the cardiovascular system at high levels, especially in the heart and caudal venous plexus, suggesting a significant role in the cardiovascular system.

Additionally, upon analyzing the Atlas for Zebrafish Development dataset, we have identified that *crip2* is expressed in specific cell lineages of zebrafish, particularly in vascular endothelial cells, skeletal muscle, notochord and cardiac muscle (Fig. S1A). Furthermore, from Daniocell dataset, we found that *crip2* is also expressed in the cell clusters such as hematopoietic/vasculature, muscle (Fig. S1B), as well as in cell clusters including vasculature, somites, notochord and heart (Fig. S1C). These findings are consistent with the WISH results, collectively indicating that *crip2* is indeed expressed in the vascular endothelial cells.

To investigate the expression of Crip2 during the early development of zebrafish embryos, we developed a *crip2* transgenic zebrafish strain driven by its native promoter sequence. Fluorescence analysis of *Tg(crip2:crip2-eGFP)* zebrafish revealed that Crip2 was expressed primarily in the lumen of the posterior main vein and the initial bud of the posterior main vein to the intersegmental vein at 26 hpf (Fig. 1M). At 50 hpf, Crip2 expression was observed in the lumen of the posterior main vein and intersegmental vein (Fig. 1N). These findings were consistent with the previous WISH results. Therefore, we speculated that Crip2 may play a role in several physiological processes in endothelial cells, including the development and formation of the lumen formation of the posterior cardinal vein and caudal vein plexus, as well as the initial sprouting and lumen formation of the intersegmental vein.

The subcellular localization of a protein has implications for its functions and potential mechanisms. By transfecting *pcDNA3.1-crip2-eGFP*, we observed that zebrafish Crip2 is localized to the cytoskeleton and extracellular pseudopodia filaments of HUVECs and that it colocalizes with F-actin (Fig. 1O, Fig. S2B, C). Additionally, we conducted immunofluorescence staining using a human CRIP2 antibody to visualize the localization of endogenous CRIP2 in HUVECs. CRIP2 was predominantly distributed in the cytoplasm and associated with the cytoskeleton and extracellular filopodia filaments (Fig. S2D). At higher magnification, CRIP2 was also observed at the cell-cell junctions, specifically within

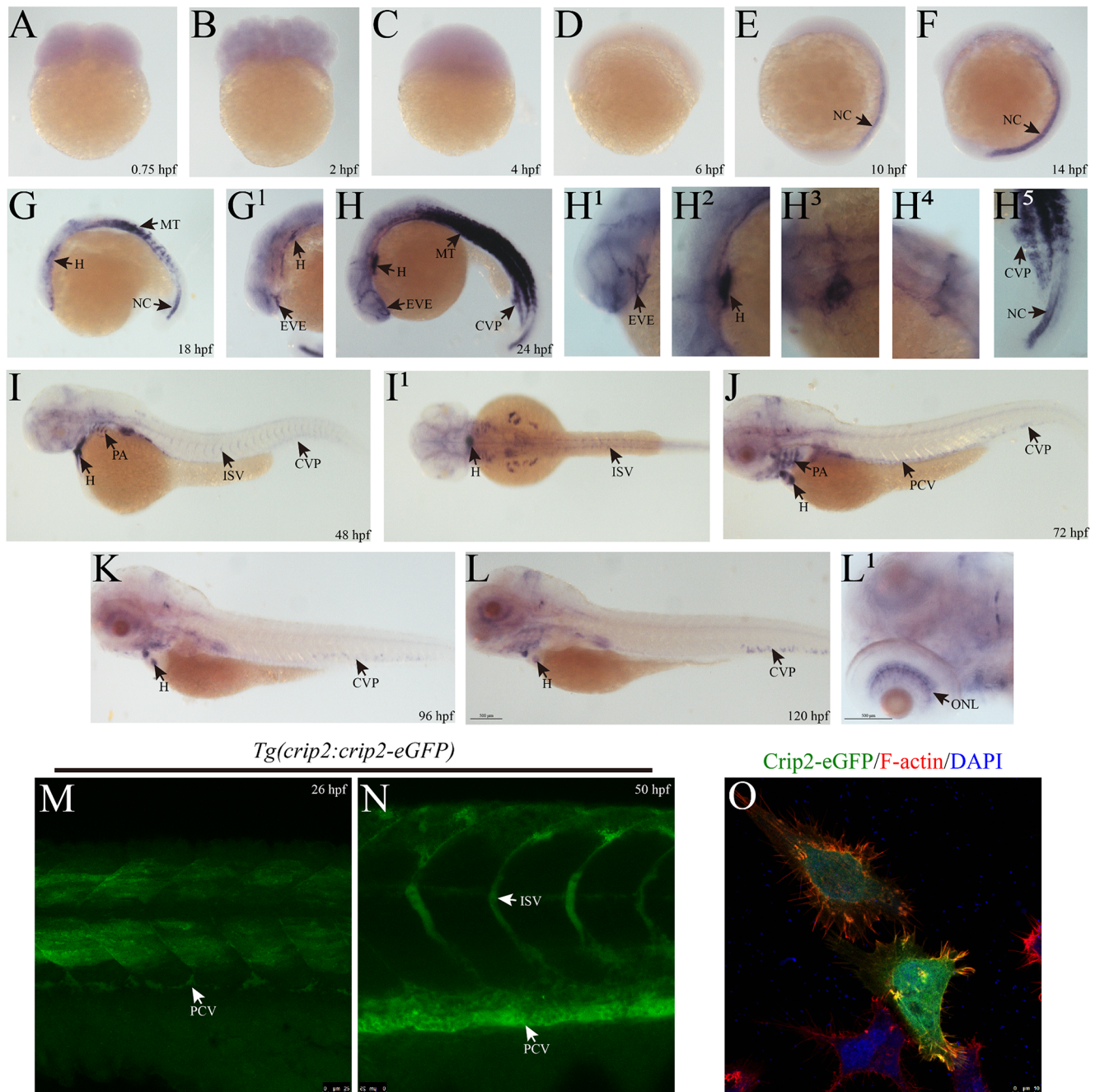


Fig. 1 The expression profiles of zebrafish *Crip2* during early vascular development. (A–L) Expression of *crip2* determined via WISH in zebrafish early embryos. The figure marked with numbers in the upper right corner is a partial enlargement of the corresponding region. (M–N) Expression of *Crip2* in early embryonic blood vessels of *Tg(crip2:crip2-eGFP)* zebrafish. The zebrafish transgenic line was constructed by expressing the *Crip2-eGFP* fusion under the control of the promoter region of *crip2*. Z-axis photography was performed,

and the target areas were superimposed. (O) Subcellular localization of *Crip2* in zebrafish via the transfection of *pcDNA3.1-crip2-eGFP* in HUVECs. TRITC-phalloidin and DAPI were used to stain F-actin and the nucleus, respectively. NC: notochord; MT: myotome; H: heart; EVE: eye blood vessel endothelial cell; CVP: caudal vein plexus; ISV: intersegmental vein; PA: pharyngeal arch; PCV: posterior cardinal vein; ONL: outer nuclear layer. hpf: hours post fertilization

the plasmodesmata (Fig. S2E, F). In summary, our findings suggest that Crip2, which colocalizes with F-actin, is located within the cytoskeleton, pseudopod filaments and plasmodesmata. This localization implies that Crip2 may play a role in the formation and function of these structures, potentially contributing to certain cellular activities dependent on them.

Deficiency of Crip2 in zebrafish affects the normal development of blood vessels

To elucidate the role of Crip2 in embryonic vascular development, we generated a zebrafish *crip2* mutant line via CRISPR/Cas9 technology. Specifically, we synthesized a sgRNA targeting the second exon of the zebrafish *crip2* gene and co-injected it with commercial Cas9 proteins into the embryos together (Fig. S3A). Following breeding and screening, we established *crip2* homozygous mutant zebrafish with a deletion of 5 indels (Fig. S3B–D). This mutation resulted in the premature termination of *crip2* translation in the middle of its first domain, yielding a truncated protein consisting of only 45 amino acids in the mutant (Fig. S3C). To assess the *crip2* mRNA and protein expression levels in the mutant zebrafish, we used qRT-PCR, RT-PCR and Western blotting. The *crip2* mRNA levels in the mutant zebrafish were reduced to approximately 10% of those in the wild-type zebrafish (Fig. S3E, F), which may be due to nonsense-mediated mRNA decay. Western blotting further confirmed that the protein expression of Crip2 significantly decreased, which corresponded to the lowest observed mRNA levels (Fig. S3G). These results collectively indicate that we have successfully established a *crip2* mutant zebrafish line.

Tal1 (also known as SCL) induces the transition of mesoderm to hematopoietic and endothelial fates in zebrafish, and its loss leads to the disorganization of major blood vessels [55–57]. Tie1 is involved in blood vessel development and endothelial cell-cell adhesion [58], and Flt1 is involved in angiogenesis and positive regulation of DNA-binding transcription factor activity [59]. To investigate the impact of Crip2 deficiency on zebrafish vasculature, we conducted WISH. Compared with that of the WT, the expression of *tal1* in the posterior cardinal vein and caudal vein plexus of the *crip2* mutants was significantly greater (Fig. 2A, B). Although qRT-PCR revealed only minor differences in the relative expression levels of *tie1* and *flt1* (Fig. 2D, F), the WISH results revealed that the lumens of the embryonic posterior cardinal vein in the mutants appeared wider, more loosely structured, intermittent and more diffuse than those in the controls did (Fig. 2C, E). In addition, there was a marked increase in the number of Flt4-positive cells in the posterior cardinal vein plexus and caudal vein plexus in the *crip2* mutants, with higher expression levels than

those in the wild type (Fig. S4A–F). These findings suggest that *crip2* mutation may lead to impaired development of the posterior cardinal vein plexus and caudal vein plexus, resulting in a diffuse and loosely organized vasculature, potentially because of reduced cell proliferation.

To investigate the cause of the hypoplasia of the posterior cardinal vein and caudal vein plexus in the mutant, we employed confocal microscopy to observe and document the mutant embryos meticulously. Our analysis revealed atypical nuclear clumping within the posterior cardinal vein and caudal vein plexus of *crip2* mutant embryos (Fig. 3A–H). Interestingly, we also observed abnormal nuclear aggregates in the notochord of the mutant embryos (Fig. S4G–I), indicating that Crip2 deficiency might lead to aberrant cell aggregation. These findings suggest that the hypoplasia observed in the posterior cardinal vein and caudal vein plexus of *crip2* mutants could be attributed to the aberrant proliferation and aggregation of endothelial cells.

CRIP2 loss increases HUVECs adhesion but reduces migration and proliferation

HUVECs are extensively used in vascular studies. To explore the mechanism of Crip2 in zebrafish vascular endothelial cell aggregation, we established human *CRIP2* mutant lines via lentivirus transfection in HUVECs. We identified two target sites on the *CRIP2* locus and two control target sites on the human *ROSA26* locus, resulting in the generation of MT1, MT2 and control cell lines (Fig. S5A, B). After screening for stable monoclonal cell lines, the expression of *CRIP2* was significantly reduced in the MT1 and MT2 lines (Fig. S5C).

Our findings suggest that the aberrant aggregation observed in zebrafish endothelial cells might be due to increased cell adhesion and/or decreased cell migration. To test this hypothesis, we first evaluated whether *CRIP2* depletion enhances cell adhesion. Compared with those in the control groups, quantitative analysis of cell attachment revealed a substantial increase in the number of adherent MT1 and MT2 cell lines. Specifically, the number of adherent cells per microscope field for the control groups was 224 ± 38 , 368 ± 34 and 646 ± 60 cells at 30, 60 and 120 min, respectively. In contrast, the values of the MT1 groups were 523 ± 30 , 721 ± 30 and 1029 ± 100 cells, representing 234.14%, 196.19% and 159.36% of those of the control groups, respectively. The MT2 groups presented adherent cell counts of 376 ± 21 , 501 ± 32 and 755 ± 90 cells, corresponding to 168.09%, 132.20% and 116.88% of the control group values, respectively (Fig. 4A, B). These data suggest that human *CRIP2* deficiency promotes the adhesion of HUVECs.

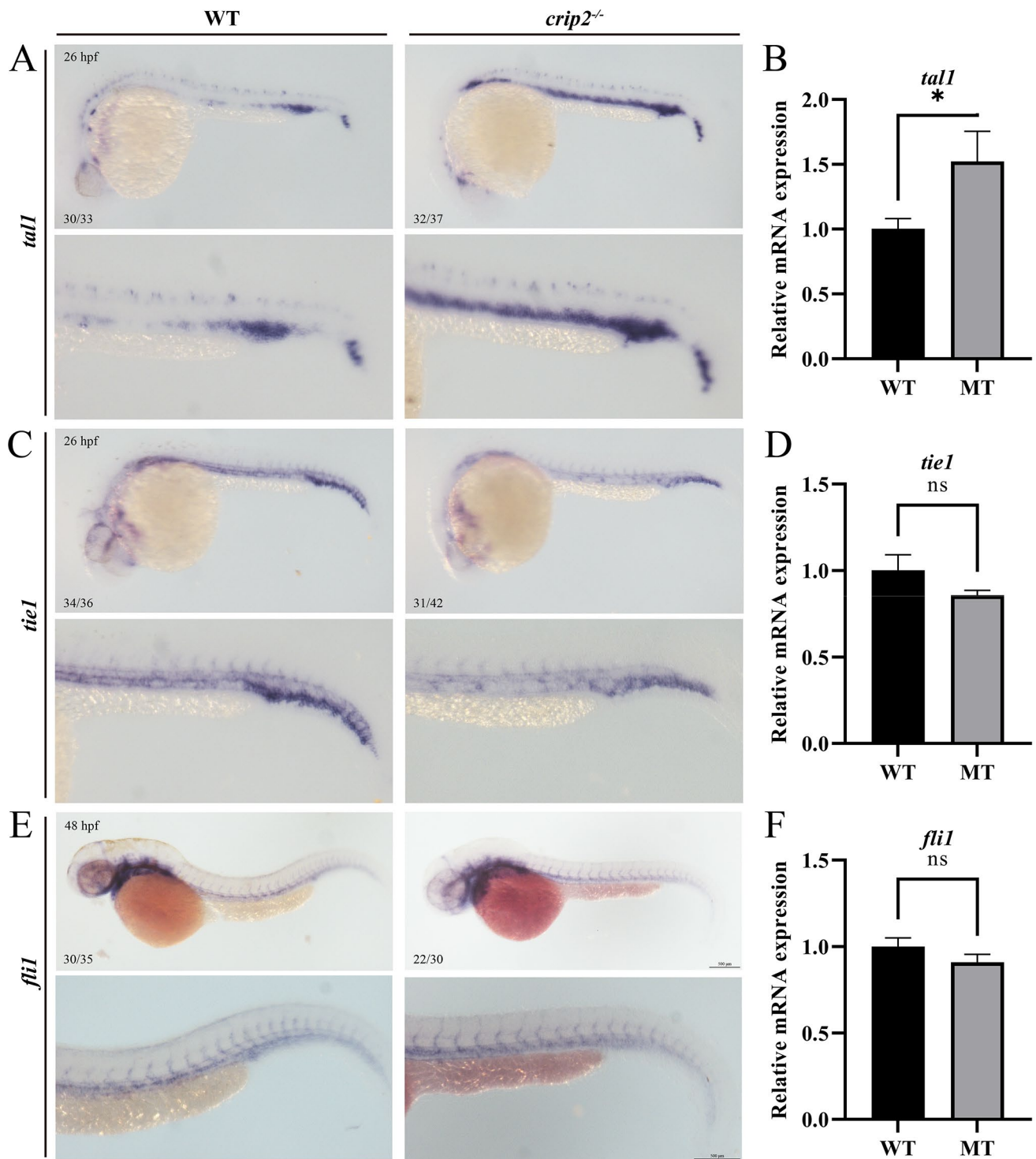


Fig. 2 Disruption of *crip2* impairs vascular development. (**A**, **C**, **E**) The expression profiles of the vascular markers, *tal1*, *tie1*, and *flil* were examined via WISH. (**B**, **D**, **F**) The relative mRNA expression

levels of these genes were detected via qRT-PCR. Unpaired *t*-test; *, $P < 0.05$; ns, not significant

The process of cancer metastasis is accompanied by changes in the adhesion ability of tumor cells [22]. To determine whether cell aggregation is a consequence of aberrant cell migration, we investigated the modulatory effect of

CRIP2 deficiency on the migration of HUVECs via a scratch assay. The results demonstrated that mutation of CRIP2 slowed the migration of both MT1 and MT2 cells toward the scratch (wound), which in turn delayed wound closure

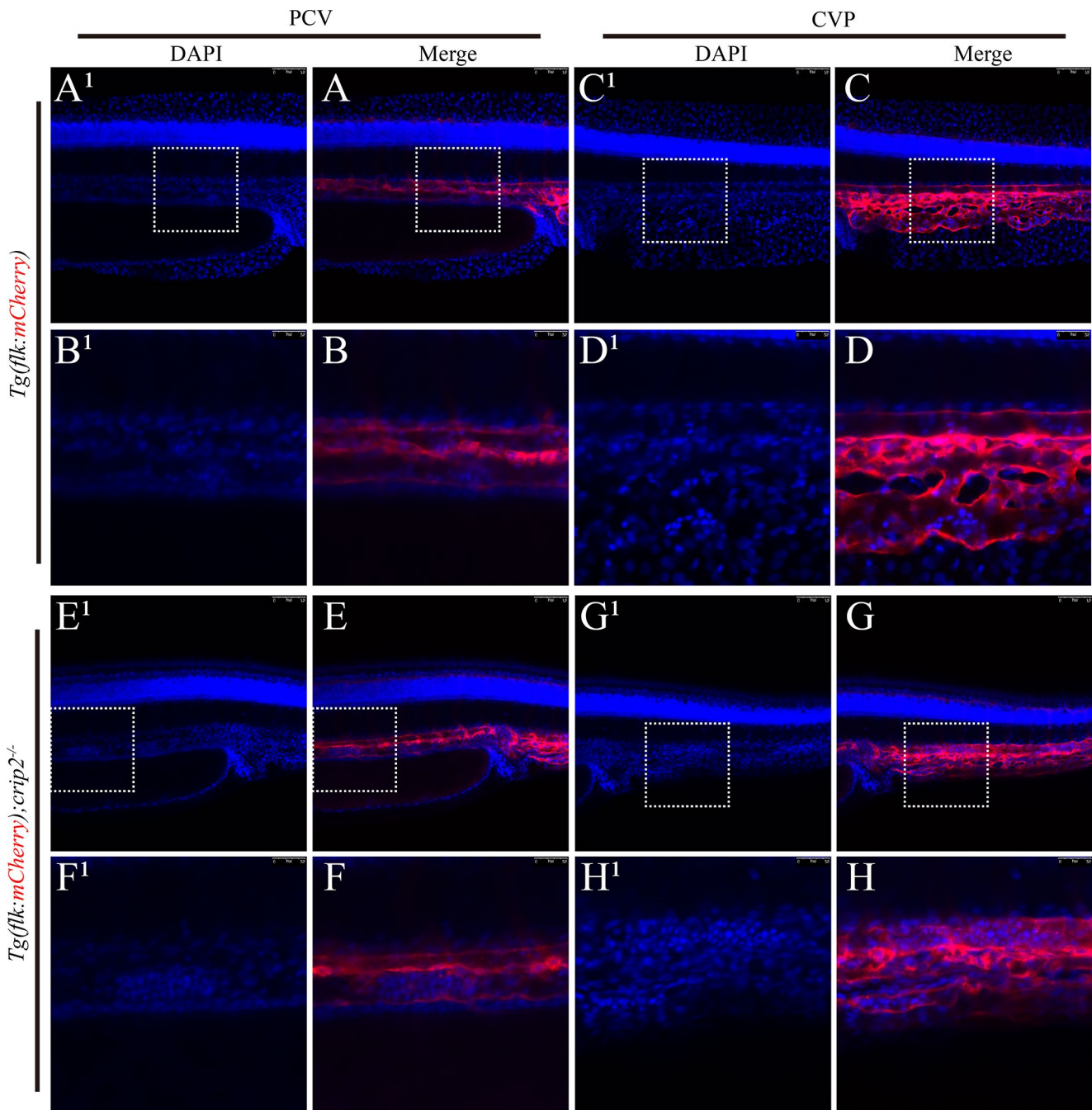


Fig. 3 Loss of CRIP2 leads to aggregation of vascular endothelial cells. No endothelial cell aggregation was observed in the PCV (A, B) or CVP (C, D) of *Tg(flk: mCherry)* zebrafish embryos at 48 hpf. Aggregation of vascular endothelial cells was observed in the PCV (E, F) and CVP (G, H) of *Tg(flk: mCherry); crip2^{-/-}* homozygous mutant embryos at 48 hpf. The embryos were stained with DAPI for nuclear

visualization, with the left panel showing the embryonic trunk and the right panel showing the embryonic tail bud. The white dashed boxes indicate the areas that are magnified in the corresponding enlarged images located below in the figures. PCV: posterior cardinal vein; CVP: caudal vein plexus

(Fig. 4C). Quantification of the wounded area revealed that MT1 and MT2 cells migrated significantly slower toward the wounded area than the control cells did, with repair rates of approximately 43.44%, 51.17% and 73.82%, respectively

(Fig. 4D). These findings suggest that CRIP2 loss impairs the migration of HUVECs.

Cell proliferation can lead to the formation of uniform and size-controlled cell aggregates [60, 61]. To explore whether cell aggregation was a result of excessive cell proliferation,

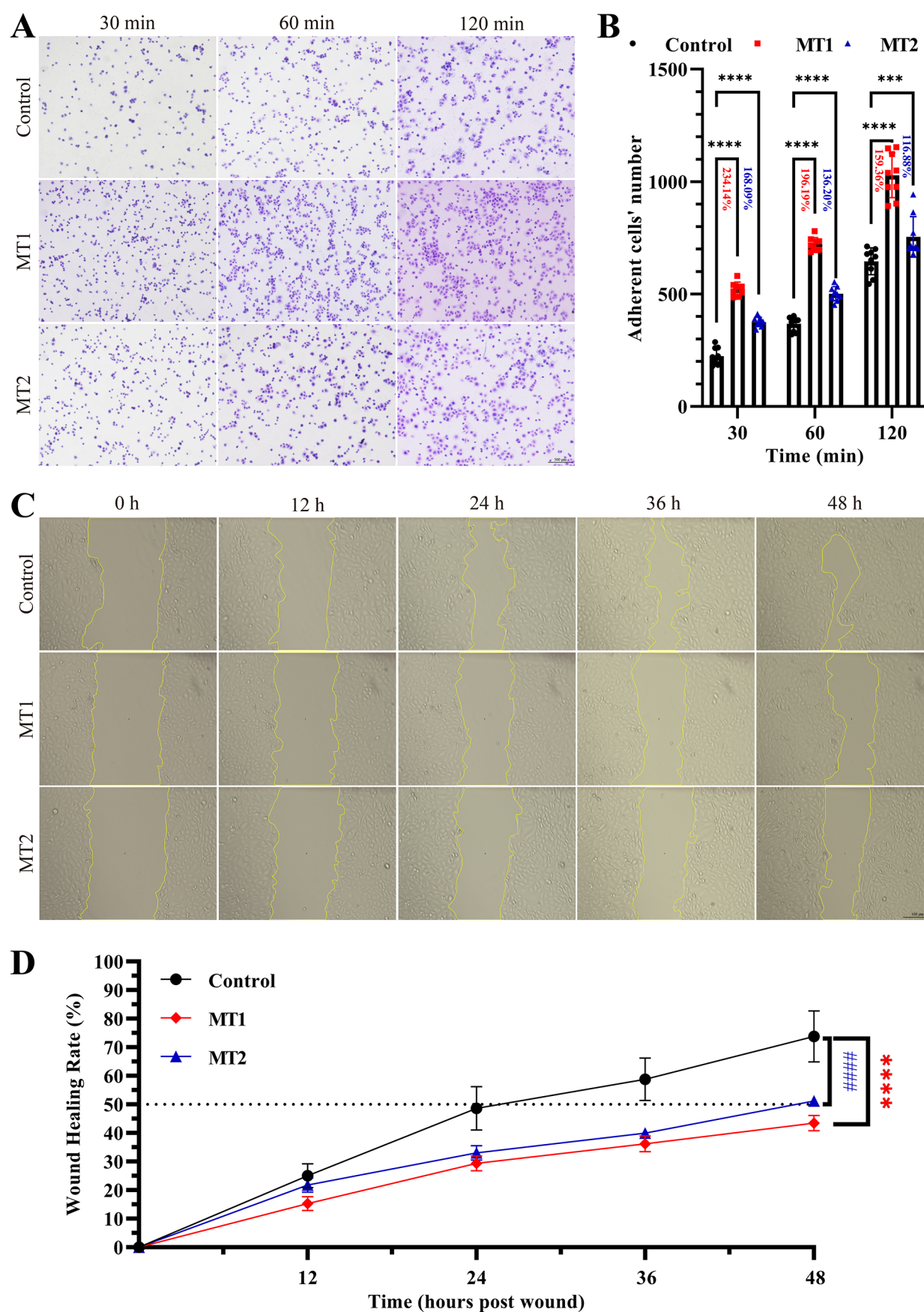


Fig. 4 CRIP2 deficiency promotes cell adhesion and impairs cell migration in HUVECs. **(A)** CRIP2 loss promotes cell adhesion. HUVECs were collected and seeded onto fibronectin-coated plates for 30, 60, or 120 min. The cells were stained with crystal violet. The adherent cells were counted via ImageJ. **(B)** Quantitative analysis of cell adhesion in *CRIP2*-MT and control cell lines. Nine microscope fields from each group were randomly captured. The percentages represent the ratios of the number of adherent cells in the *CRIP2*-MT cell lines to that in the control groups. **(C)** CRIP2 loss impairs cell migration. HUVECs were collected, seeded and photographed at 0, 12, 24, 36, and 48 h after wounding. Wound closure was investigated via ImageJ. **(D)** Quantitative analysis of cell migration in *CRIP2*-MT and control cell lines. Six microscope fields from each group were randomly captured. Two-way ANOVA; ##### or *****, $P < 0.0001$

we measured the proliferation of three cell lines by assessing DNA biosynthesis. We found that the proportion of EdU-positive HUVECs relative to the total number of cells in the MT1 and MT2 cell lines was substantially lower than that in the control cells (Fig. 5A), accounting for approximately 53.81% and 66.74% of the total number of MT1 and MT2 cells, respectively, compared with 86.06% of the control cells (Fig. 5B). These findings suggest that CRIP2 deficiency inhibits the proliferation of these cells. Cell proliferation was reduced, but did cell apoptosis increase as a consequence? To explore the effect of CRIP2 on cell death, we conducted a TUNEL assay. The assay revealed no detectable apoptotic signal in these cells compared with a positive control that had been treated with DNase I (Fig. S5D). Collectively, these findings indicate that the loss of CRIP2 leads to functional alterations in HUVECs, characterized by increased adhesion and decreased migration and proliferation. These changes contribute to the aberrant aggregation of endothelial cells during embryonic vascular development in zebrafish.

CRIP2 prevents hyper-adhesion by fine-tuning the cytoskeleton

The process of cell aggregation relies on cell adhesion proteins [17], which facilitate more compact aggregation via cell-cell interactions, including cell adhesion and cell junctions [62, 63]. To delve deeper into the molecular mechanisms responsible for this cell adhesion phenotype, we conducted a detailed examination of cell junctions. ZO-1, a protein integral to tight junctions [64], was found to be upregulated in MT1 and MT2 cells compared with the control group. Additionally, the expression pattern of ZO-1 was distorted, suggesting that the tight junctions of HUVECs were strengthened due to CRIP2 loss (Fig. 6A, C). The expression of vinculin, a molecule associated with cell-matrix adhesion and F-actin, helps to define the cytoskeleton and the structural morphology of cells. The immunostaining results revealed that the adhesion of MT1 and MT2 cells was significantly greater than that of the control

cells (Fig. 6B). Moreover, the colocalization of F-actin and Vinculin in MT1 and MT2 cells highlighted the formation of Vinculin-based focal adhesions, and Vinculin-based adhesion stress fibers were clearly evident, a feature not present in the control groups (Fig. 6B, D). Similarly, the expression of CD31 and E-cadherin (also known as CDH1), the primary components of cell-cell adhesion, was significantly increased compared with that in the control groups (Fig. 6E, F). These observations suggest that the loss of CRIP2 resulted in a hyperadhesive HUVEC phenotype, thereby enhancing cell aggregation.

Many studies have demonstrated that LIM domains play crucial roles in mediating protein-protein or protein-DNA interactions, which are essential for the biological functions of numerous LIM proteins [65]. To further investigate the mechanisms underlying hyperadhesion, we identified potential proteins that interact with CRIP2 through immunoprecipitation via the use of a Flag antibody in CRIP2-Flag overexpressing HUVECs. In addition to the light and heavy chain bands, several other bands were precipitated by the Flag antibody. Notably, a prominent band ranging from 50 to 70 kDa was observed and selected for mass spectrometry analysis (Fig. 7A). The most abundant protein identified with the highest score was K2C8, also known as KRT8 (Fig. S6A). The relative molecular mass of KRT8 was approximately 56.6 kDa, which corresponded well with the size of the band used for mass spectrometry analysis. KRT8, a type II keratin, forms intermediate fibers in epithelial cells and is involved in the maintenance of cell structural integrity, signal transduction, and cell differentiation [66, 67].

To validate the interaction between KRT8 and CRIP2, we employed a KRT8 antibody for Western blot analysis of the Flag immunoprecipitation products from CRIP2-Flag overexpressing cell lines. KRT8 was detected in the immunoprecipitation products (Fig. 7B), confirming that human CRIP2 and KRT8 can indeed bind to each other. Total proteins were subsequently extracted from cells cotransfected with *pCMV-CRIP2-C-Flag* and *pCMV-KRT8-C-HA*, followed by coimmunoprecipitation using Flag and HA antibodies, respectively. In the immunoprecipitation products, a distinct band corresponding to the relative molecular mass of KRT8 or CRIP2 was clearly visible (Fig. 7C). These findings further support the interaction between CRIP2 and KRT8.

In addition, mass spectrometry analysis revealed that vimentin (also referred to as VIM) is a protein that interacts with CRIP2, with its score and abundance ranking third (Fig. S6A). VIM, a type of class III intermediate filament, is found in various nonepithelial cells, particularly mesenchymal cells, and plays a critical role in stabilizing the cytoplasmic architecture [68]. To confirm the interaction, the VIM antibody was used for Western blot analysis of the immunoprecipitation products, which confirmed that

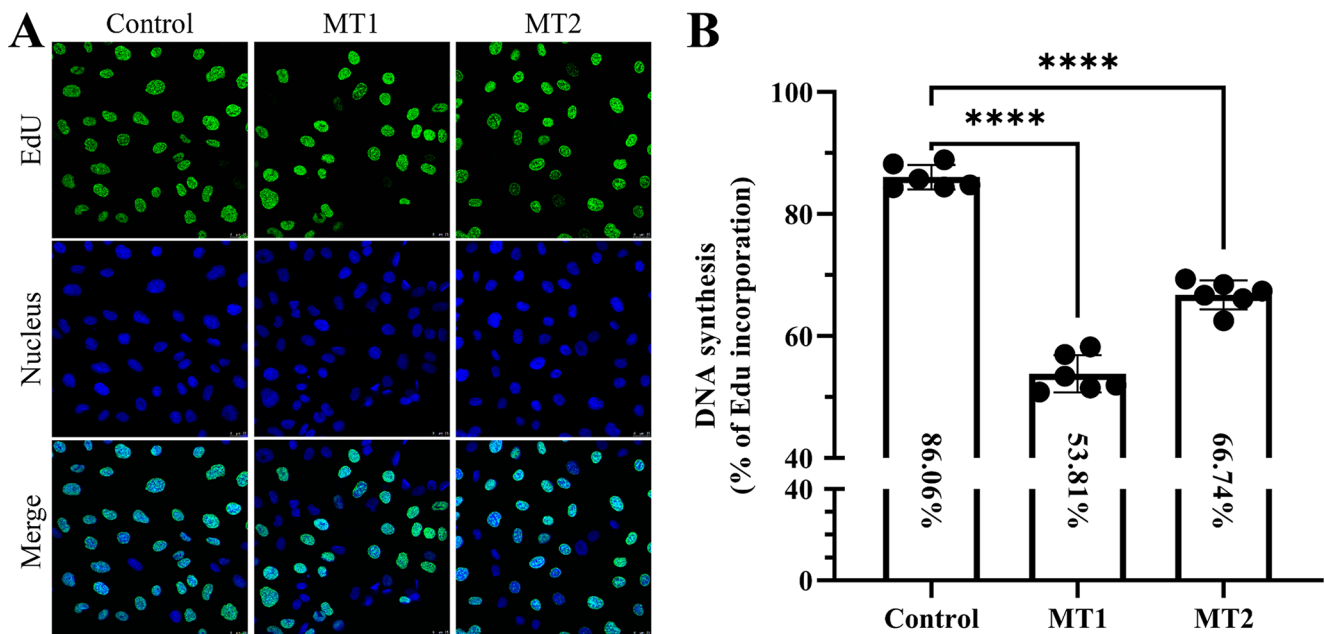


Fig. 5 CRIP2 depletion decreases cell proliferation in HUVECs. **(A)** CRIP2 loss reduces cell proliferation, as determined by the EdU assay. Ten microscope fields from each group were randomly captured. The proliferative cells were counted via ImageJ. **(B)** Quantitative analysis of cell proliferation in *CRIP2*-MT and control cell lines. Six micro-

scope fields from each group were randomly captured. The percentages represent the ratios of the number of EdU-positive cells to the total number of cells in the control and the MT1 and MT2 cell lines. One-way ANOVA; ****, $P < 0.0001$

VIM was indeed an interacting protein of CRIP2 (Fig. S6B). Moreover, a distinct band corresponding to the relative molecular mass of VIM or CRIP2 was evident in the immunoprecipitation products that were coimmunoprecipitated from HEK293T cells following cotransfection with *pCMV-CRIP2-C-Flag* and *pCMV-VIM-C-HA* (Fig. S6C). Our previous results revealed that zebrafish Crip2 colocalizes with F-actin and is localized to the cytoskeleton. On the basis of these observations, we hypothesized that CRIP2 binds to cytoskeletal proteins, thereby regulating cell behavior.

KRT8 affects the adhesion and permeability of tight junctions and regulates cell-matrix adhesion via integrins when its expression is elevated [69, 70]. FRMD3 can interact with vimentin to induce the degradation of vimentin, which in turn downregulates the proteins of the focal adhesion complex [71]. We investigated the expression of KRT8 and VIM in the context of CRIP2 loss. Compared with that of the control group, the fluorescence of KRT8 was more intense, and the keratin intermediate filaments in the cytoskeleton appeared more irregular (Fig. 7D). Similarly, the fluorescence of F-actin indicated cytoskeletal hyperplasia following CRIP2 deficiency (Fig. 7E), which aligns with previous findings. Additionally, the expression of KRT8 was upregulated in the absence of CRIP2 and downregulated with CRIP2 overexpression, indicating a negative correlation between CRIP2 and KRT8 expression (Fig. 7F, G). Similarly, the fluorescence of VIM revealed a disordered, proliferous and polydirectional cytoskeleton, with VIM

upregulated in the absence of CRIP2 (Fig. 7H, Fig. S6D). In summary, KRT8 and VIM were upregulated in the context of CRIP2 deficiency, leading to a hyperplastic cytoskeleton and the formation of hyperadhesion. These observations indicate that CRIP2 fine-tunes cytoskeleton formation by negatively regulating the expression of KRT8 and VIM, thus controlling the normal formation of cell adhesion.

CRIP2 maintains normal cell movement through the VEGFA/CDC42 signaling pathway

The VEGFA/CDC42 signaling pathway is a well-known pathway that regulates cell proliferation, colony formation, migration and invasion [72]. We investigated whether the VEGF-CDC42 signaling pathway was interrupted following the loss of CRIP2. We observed that the fluorescence of VEGFA was lower in *CRIP2*-mutant cells than in control cells (Fig. 8A). Additionally, VEGFR, the receptor of VEGFA, was significantly downregulated in *CRIP2*-mutant cells compared with control cells (Fig. 8B, E). Furthermore, CRIP2 deficiency led to a marked decrease in the mRNA expression of *MAPK14* (p38- α) and *HSP27* (Fig. 8E), which are substrates, as well as a reduction in the protein expression of ECM1 (Fig. 8D).

We further examined the expression of CDC42 in *CRIP2* mutant cells. The expression of CDC42 was significantly lower in CRIP2-deficient cells than in control cells (Fig. 8C). Additionally, WASP, the effector through

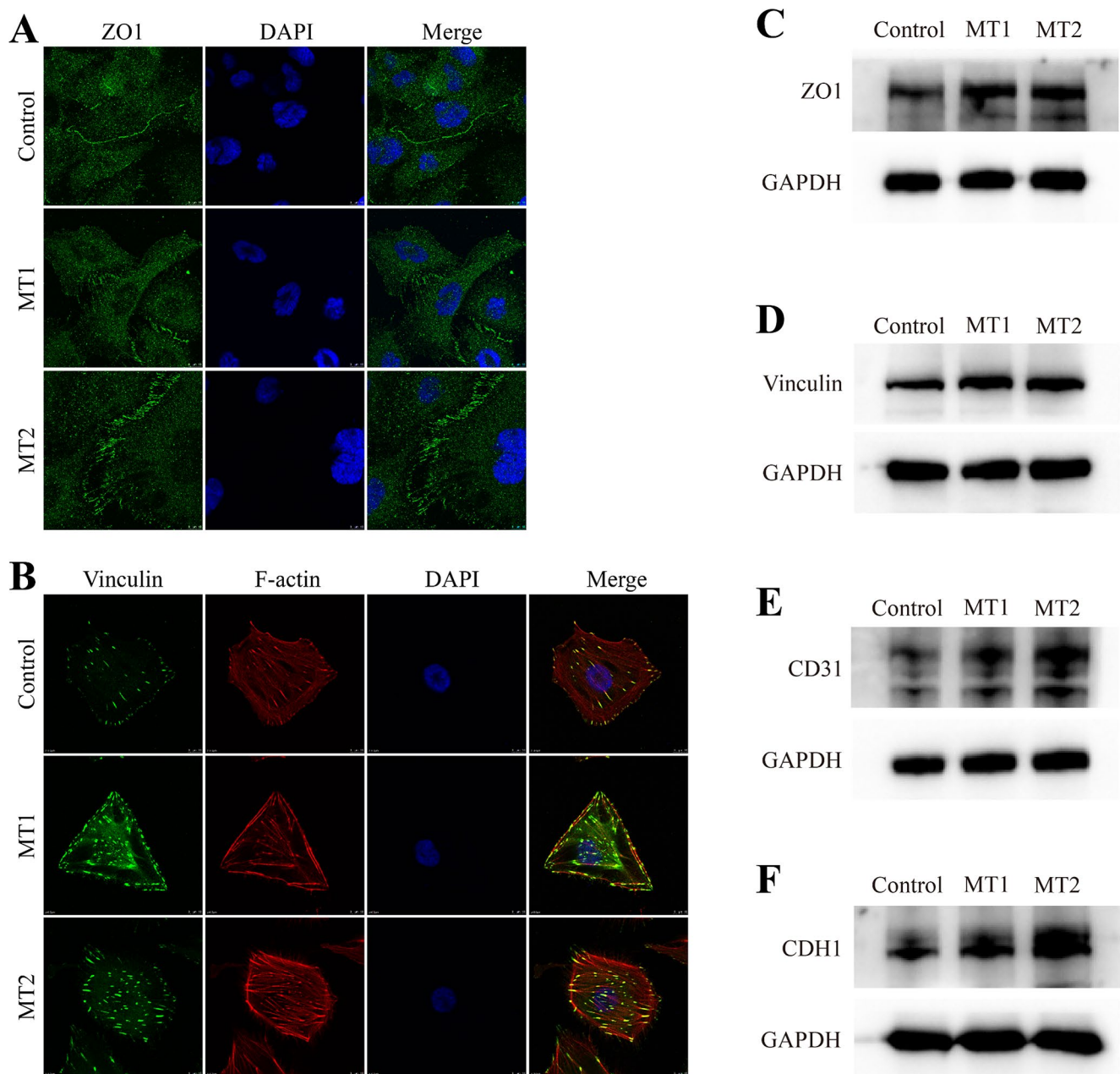


Fig. 6 Cell adhesion proteins are upregulated following CRIP2 depletion. (A–B) ZO1 and Vinculin expression in the control and *CRIP2*-MT cell lines were determined by immunostaining. TRITC-phalloidin

and DAPI were used to stain F-actin and the nucleus, respectively. (C–F) ZO1, vinculin, CD31 and CDH1 expression in the control and *CRIP2*-MT cell lines, as determined by Western blotting

which CDC42 controls polarity for efficient chemotaxis and transmigration, was also notably decreased (Fig. 8F). qRT-PCR revealed that the mRNA expression levels of CDC42 effectors, including *MRCK*, *MLC2* and *PAK2*, were substantially lower than those in the control group (Fig. 8F). Furthermore, the mRNA levels of *TWIST1* and *MMP2*, downstream factors of Cdc42, were also significantly lower in *CRIP2*-mutant cells than in control cells. These findings indicate that CRIP2 deficiency disrupts the VEGFA/CDC42

signaling pathway, leading to a decrease in the migration of HUVECs.

CRIP2 sustains cell proliferation via PDE10A/cAMP signaling and PDGF/JAK/STAT/SRF signaling

To explore the molecular mechanisms of decreased proliferation in CRIP2-deficient cells, we conducted transcriptome sequencing (RNA sequencing [RNA-seq]) to identify the differentially expressed genes (DEGs) between the control

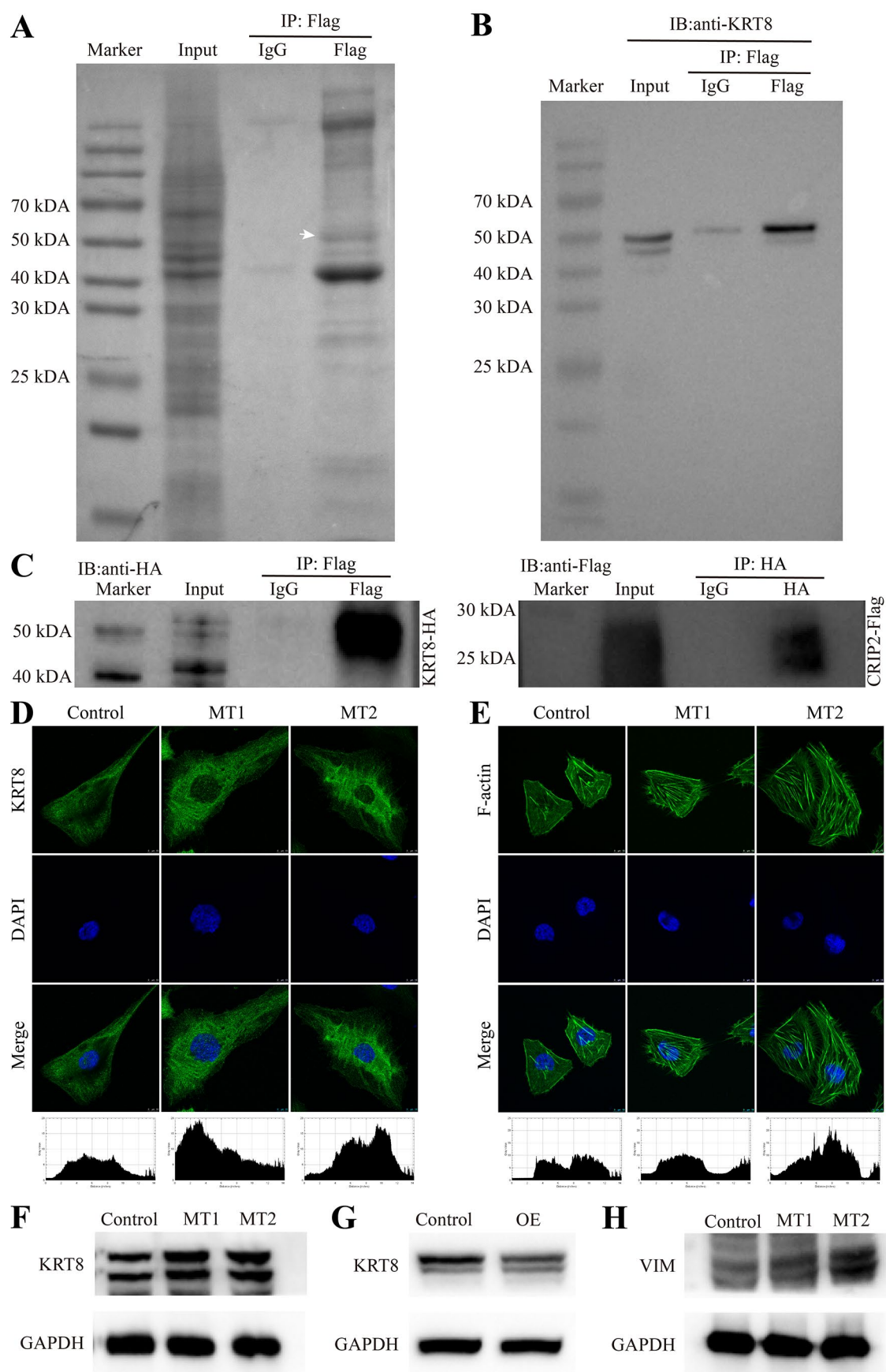


Fig. 7 KRT8 interacts with CRIP2 and is negatively regulated by CRIP2. **(A)** Identification of potential CRIP2-interacting proteins by immunoprecipitation using a Flag antibody in CRIP2-Flag-over-expressing cell lines. The white arrow indicates the bands for mass spectrometry sequencing. **(B)** Validation of the interaction between KRT8 and CRIP2 via KRT8 antibody immunoblotting. **(C)** CRIP2 coimmunoprecipitates with KRT8. **(D, E)** The expression of KRT8 and F-actin in the absence of CRIP2. DAPI was used to stain the nucleus. Below the images are the fluorescence intensity analysis data. The x-axis represents the horizontal distance across the image from left to right, whereas the y-axis represents the gray value corresponding to the fluorescence intensity. **(F)** KRT8 expression in the absence of CRIP2, as determined by Western blotting. **(G)** KRT8 expression following CRIP2 overexpression, as determined by Western blotting. **(H)** Western blot analysis of Vimentin expression in the absence of CRIP2

and *CRIP2*-mutant cells. Compared with the control cells, the MT1 cells presented 134 DEGs, with 59 downregulated and 75 upregulated genes. In MT2 cells, we identified 720 DEGs, of which 468 were downregulated and 252 were upregulated (Fig. S7A, B). Notably, *PDE10A* was among the genes whose expression was most significantly downregulated (Fig. S7A-D). Subsequent immunofluorescence and Western blot analyses confirmed that the fluorescence, mRNA and protein levels of *PDE10A* were significantly reduced following the loss of CRIP2 (Fig. 9A, D; Fig. S8D). *PDE10A*, which can hydrolyze both cAMP and cGMP, plays a role in SMC proliferation and intimal hyperplasia by at least partially antagonizing CNP/NPR2/cGMP/PKG1 α signaling [73]. The expression of PKG1 β , an isoform of PKG1 generated by alternative splicing whose activation promotes SMC proliferation, was also significantly decreased at the mRNA level (Fig. S8D). Protein kinase A (PKA), an effector of cAMP, inhibits VSMC proliferation by remodeling the actin cytoskeleton and modulating the activity of serum response factor (SRF), which in turn regulates the expression of genes essential for proliferation [74]. The KEGG enrichment scatter plot for DEGs in CRIP2-deficient cell lines revealed that the cAMP signaling pathway was significantly enriched, ranking among the top 20 signaling pathways (Fig. S7E, F). Furthermore, within the cAMP signaling pathway, the mRNA expression of *PRKACA* and *PRKACB*, members of the PKA family, and their downstream gene *GLII*, a key effector in the Hh signaling pathway, significantly decreased. Conversely, *F2R* (also known as *PAR1*), which promotes the formation of cortical actin caps and influences actin cytoskeletal organization, was significantly upregulated (Fig. S8A, B, D). These findings indicate that *PDE10A*/cAMP signaling plays a role in regulating cell proliferation in the absence of CRIP2.

The PDGF/PDGFR signaling pathway is known to play a pivotal role in cancer proliferation, metastasis, invasion, and angiogenesis by modulating multiple downstream pathways; one such pathway involves PDGF signaling through SRF, which drives a proliferation program at the midface

[75]. SRF is also a downstream target of cAMP signaling and has been identified as a candidate interacting protein of human CRIP2 in the STRING dataset (Fig. S8C). Our investigation revealed that CRIP2 can bind to SRF, as evidenced by its presence in the immunoprecipitation product of CRIP2-overexpressing cell lines (Fig. 9B). In addition, upon cotransfection with *pCMV-CRIP2-C-Flag* and *pCMV-SRF-C-HA*, a distinct band corresponding to the relative molecular mass of SRF or CRIP2 was clearly observed in the immunoprecipitation products (Fig. 9C). In the *CRIP2* mutant cells, SRF protein levels were significantly downregulated (Fig. 9E), along with those of its upstream factors, PDGFB and PDGFRB, which were significantly reduced at both the mRNA and protein levels (Fig. 9F, Fig. S8D). JAK, a downstream tyrosine kinase in PDGF receptor signaling, is directly activated by PDGF to induce mitogenesis in fibroblasts [76, 77]. We found that the mRNA expression of *JAK1*, *JAK2*, *STAT1* and *STAT3*, was significantly lower in the mutants than in the controls (Fig. S8E). Similarly, the expression of *IL11* and *IL11RA*, which contribute to cancer cell survival and proliferation through JAK/STAT signaling, was also substantially reduced following CRIP2 loss (Fig. 9G, Fig. S8E). These changes resulted in a marked increase in p21 levels (Fig. 9H) and a decrease in CDK1, CDK2 and CCND2 levels (Fig. 9I, Fig. S8E), all of which are critical for cell cycle progression. These findings suggest that CRIP2, through its interaction with SRF and PDGF/JAK/STAT signaling, regulates cell proliferation.

Discussion

Crip2, a member of the Crip protein family within the LIM protein superfamily, is known for its role in tumorigenesis and cardiac development [44, 45, 78–80]. This study revealed that Crip2 is critical for vascular development in zebrafish, with its deficiency impacting embryonic vascular lumen formation. We demonstrated that CRIP2 interacts with KRT8, VIM and SRF, fine-tuning cell adhesion, proliferation and migration by modulating the adjusted cytoskeleton, VEGFA/CDC42 signaling, and *PDE10A*/cAMP and PDGF/JAK/STAT signaling, ultimately participating in vascular development.

Previous studies have shown that LIM proteins are integral to cardiovascular development, cardiomyocyte metabolism and cell differentiation. LMO7, for example, is implicated in heart development and is moderately expressed in normal vessels [81]. LMO2 is expressed in the vascular endothelium of mouse embryos and is necessary for the angiogenic remodeling of capillary networks [82]. FHL2 is highly expressed in the vascular system, including blood vessels in smooth muscle cells (SMCs) and endothelial cells

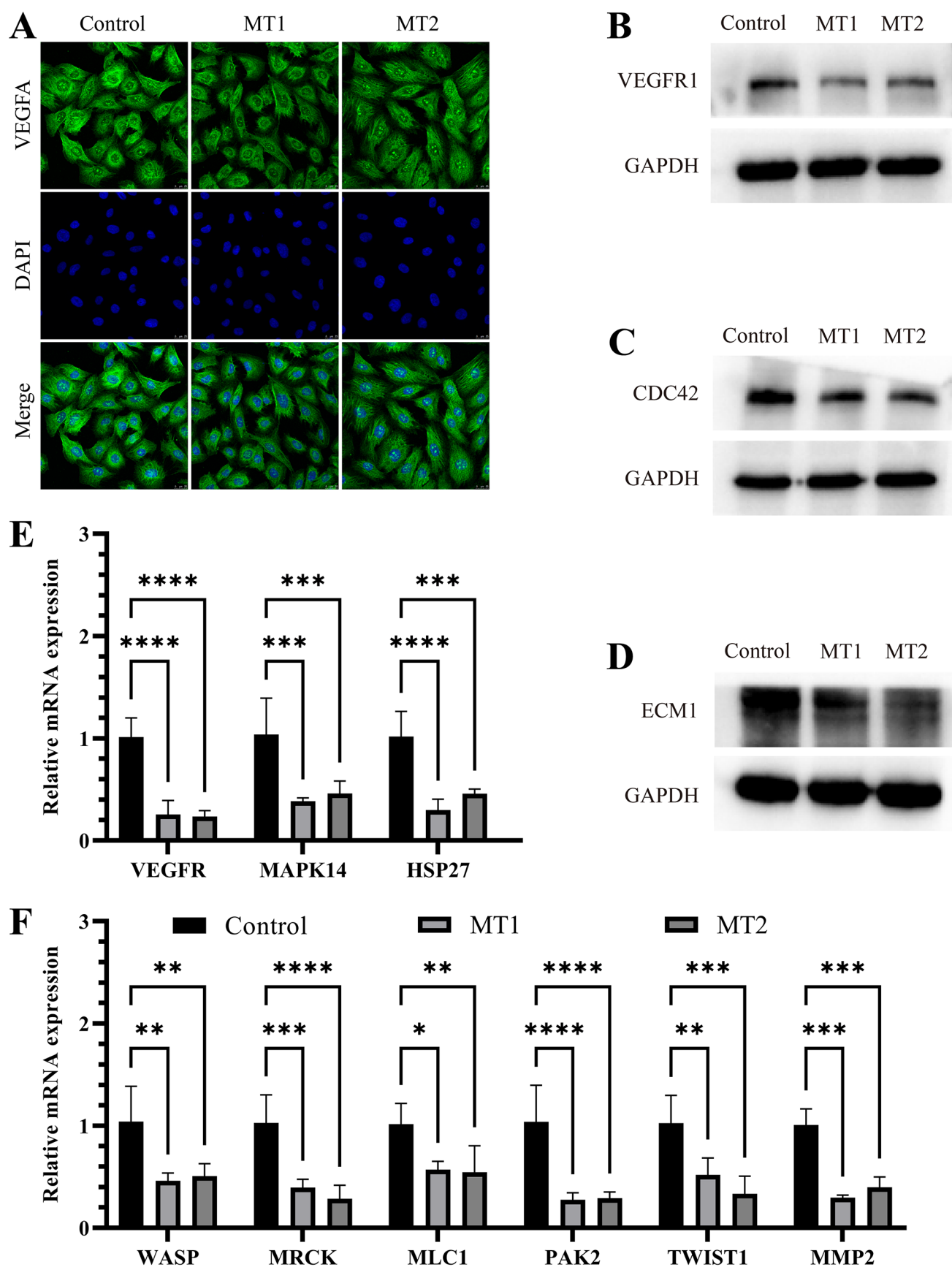


Fig. 8 CRIP2 deficiency decreases the expression of factors related to cell migration. (A) Immunofluorescence analysis of VEGFA upon CRIP2 loss. DAPI was used to stain the nucleus. (B, C, D) The protein levels of ECM1, VEGFR1 and CDC42 were diminished in CRIP2-deficient cells. (E, F) qRT-PCR revealed a reduction in the expression of factors downstream of VEGFA/CDC42 following CRIP2 loss. Two-way ANOVA; *, $P < 0.05$; **, $P < 0.01$; ***, $P < 0.001$; ****, $P < 0.0001$

[83]. In our study, both WISH and *Tg(crip2:crip2-eGFP)* transgenic zebrafish lines revealed that Crip2 is dynamically and specifically expressed during early development, with predominant expression in the cardiovascular system, especially in the vascular system. As a LIM-only protein, CRIP2 shares an expression pattern with other LIM proteins in blood vessels and endothelial cells. Consistent with these findings, Crip2 is expressed in the heart and contributes to cardiac development in both mice and zebrafish [44–46, 84]. In *Xenopus*, Crip2 is highly expressed in the cardiovascular system, brain, and neural tube [85]. Our results align with these observations, and we note that zebrafish Crip2, unlike *Xenopus* Crip2, exhibits strong maternal expression, suggesting a potential maternal contribution to development.

We found that Crip2 is crucial for blood vessel lumen formation. Crip2 depletion led to aberrant aggregation of endothelial cells and subsequent lumen hypoplasia. In recent decades, in vitro and in vivo studies have echoed these findings. CRIP2 interacts with NF- κ B/p65 and transcriptionally represses NF- κ B-mediated expression of proangiogenic cytokines, inhibiting tumor formation and angiogenesis in nasopharyngeal carcinoma cell lines [86]. This study suggests that Crip2 is involved in vascular development and that its loss leads to vascular hypoplasia. This finding aligns with findings that CRIP2 inhibits esophageal squamous cell carcinoma tumorigenesis by reducing colony formation, growth, and invasion abilities [79]. The aggregation of endothelial cells in Crip2 deficient zebrafish is consistent with earlier observations of cell clumping.

Additionally, we found that functional HUVECs exhibit enhanced adhesion and decreased proliferation and migration upon CRIP2 loss, further underscoring the importance of CRIP2 in vascular homeostasis. LIM-only proteins are known to regulate cell aggregation and proliferation. Studies have shown that MDA-MB-231 cells stably expressing CRIP2 exhibit reduced cell viability, migration, invasion, tumor growth and angiogenesis in mouse xenograft models [87]. In zebrafish, Crip2 is present in premigratory neural crest cells (NCCs) in rhombomere 6, migrating NCCs and aortic vessels in pharyngeal arches 3 to 6, and disruption of Crip2 expression leads to abnormal migration of NCCs [45]. Additionally, Lmo2 knockdown in HUVECs significantly impairs endothelial proliferation, blocks the G1/S transition, and reduces angiogenesis by decreasing transforming growth factor- β (TGF- β) expression [82]. Our results align

with these previous findings and collectively suggest that Crip2 is indeed involved in the regulation of cell aggregation and proliferation.

LIM proteins serve as adapters or scaffolds, facilitating the assembly of multimeric protein complexes [32, 33]. Our subcellular localization and immunofluorescence studies revealed that the Crip2 protein is localized primarily to the cytoskeleton, pseudopod filaments and plasmodesmata and colocalizes with F-actin. Previous research has shown that CRIP2 is distributed in the cytoplasm of olfactory precursor cells [88], and colocalizes with cardiac troponin T in the thin-filaments of sarcomeres [46] and with F-actin [89]. These findings suggest that Crip2 may exert its function through the cytoskeleton in the cytoplasm. Our study also revealed that CRIP2 fine-tunes cytoskeleton formation to control cell adhesion by interacting with KRT8 and VIM, both of which are intermediate filament proteins. LIM proteins are also known to control gene expression and cytoskeletal function. Zyxin participates in cell adhesion and migration by interacting with intermediate filaments such as Synemin (SYNM) [90]. LIMK1 and LMO1 are recruited to force-bearing keratin fibers and directly interact with stretched keratin 8/18 fibers to play diverse roles in force-regulated signaling [91]. Upon FHL2 depletion, pancreatic cancer cell lines exhibit significantly decreased cell survival and proliferation, highlighting the regulatory role of LIM proteins in the cytoskeleton [92]. Similarly, we found that CRIP2 loss upregulated the expression of ZO-1, vinculin, CD31 and E-cadherin, which are crucial for cell adhesion. The concurrent increase in adhesion capacity suggests that CRIP2 plays a pivotal role in modulating the cytoskeleton and cell adhesion.

The metastasis of cancer is closely associated with the altered adhesion properties of tumor cells [22], and impacts cell migration and movement [23]. Our findings indicate that CRIP2-deficient HUVECs exhibit reduced migration, primarily due to the downregulation of the VEGFA/VEGFR/CDC42 signaling pathways. The activation of CDC42 and the inhibition of GSK-3 β are emerging as novel strategies to correct VEGF-driven angiogenesis-related anomalies [93], and *CDC42* knockdown has been shown to inhibit the migration and proliferation of WRO cells [94]. VEGF-activated CDC42 localizes to the leading edge of migrating CRC cells, regulating directional migration, invasion, and metastasis [95]. Decreased levels of HSP27, a MAPK14 substrate, lead to F-actin polymerization and reduced cell migration [96]. CDC42, through its effector proteins, such as PAK2 and MRCK, plays crucial roles in actin dynamics, cell motility, actin-myosin regulation and apicobasal polarity. In *CRIP2* mutant cells, we observed a significant reduction in these CDC42 effectors. Additionally, ECM1 blockade dampened hEM15A cell migration and altered the

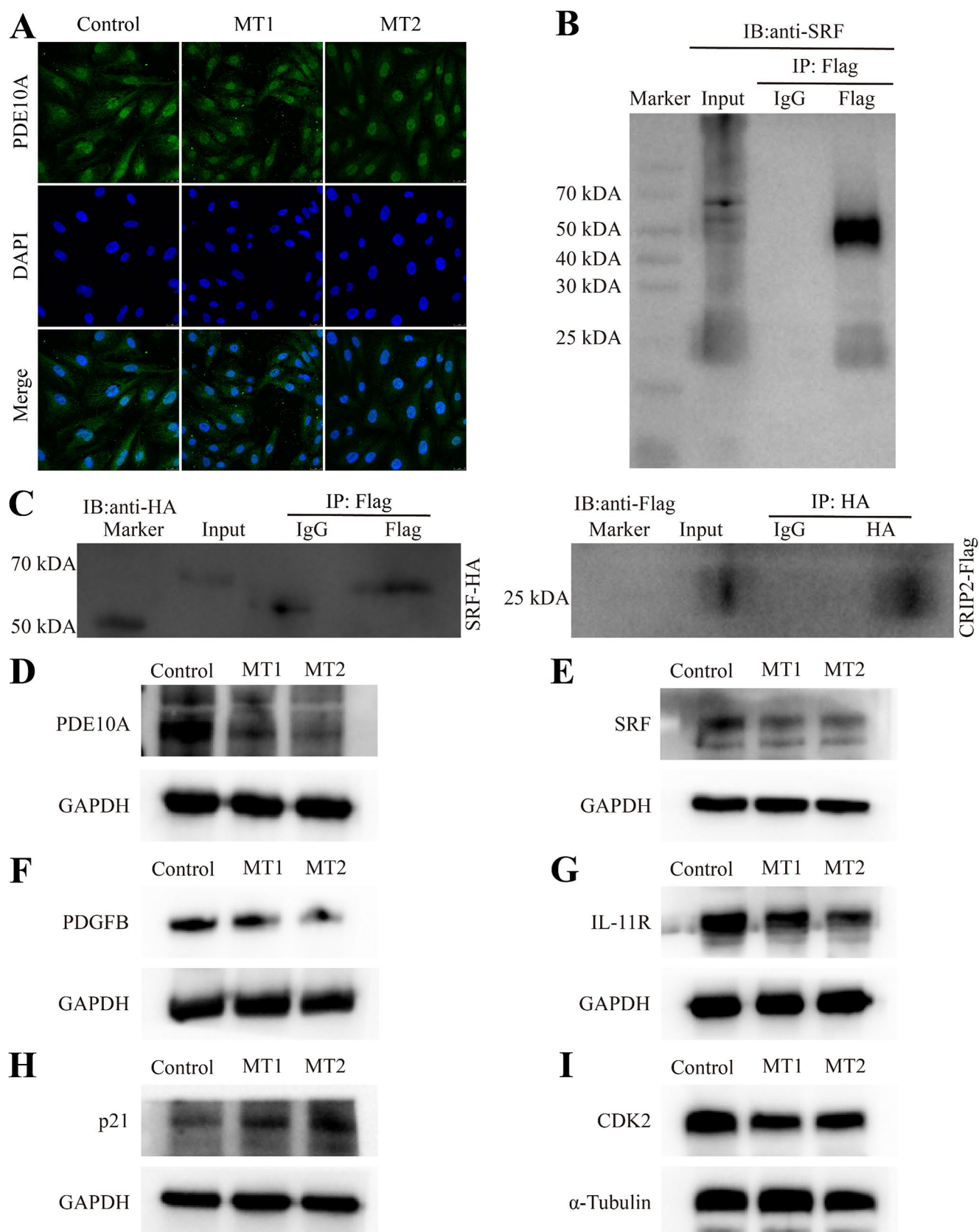


Fig. 9 SRF interacts with CRIP2, and the expression of its downstream genes is modulated by CRIP2. **(A)** Immunofluorescence analysis of PDE10A expression after CRIP2 depletion. DAPI was used to stain the nucleus. **(B)** Detection of SRF in the immunoprecipitation derived from cell lines overexpressing CRIP2. **(C)** CRIP2 coimmunoprecipitates with SRF. **(D–I)** Analysis of the altered protein levels of PDE10A, SRF, PDGFB, IL-11R, p21, and CDK2 in response to CRIP2 deficiency

F-actin cytoskeleton distribution [97]. PAK2 and MRCK are critical for cell migration and invasion, with MRCK activating myosin II by phosphorylating Ser19 of the myosin light chain (MLC) [98]. MMPs facilitate cell migration and invasion by digesting specific extracellular matrix components [99], whereas TWIST1 knockdown inhibits macrophage chemotaxis and migration through the CCL2/CCR2 axis [100]. Thus, CRIP2 deficiency affects cell migration by altering the VEGFA/CDC42 signaling pathway. Further research is necessary to elucidate the mechanisms by which CRIP2 influences this pathway.

During gastrulation, axial mesodermal cells, which are the precursors of the notochord, migrate anteriorly and populate the notochordal plate [101]. The PCP signaling pathway regulates the distribution of cytoskeleton, and its disruption leads to random directions movement of notochord cells [102, 103]. By approximately E10.5 of mouse embryos, the notochord adheres to the ventral surface of the neural tube [101]. These observations suggest that the migration and adhesion are essential processes for proper notochord development. In this study, we have discovered that *Crip2* is expressed in the notochord. The loss of *Crip2* results in abnormal nuclear aggregates in the notochord. In light of our findings that the absence of CRIP2 also impairs migration and adhesion of endothelial cells, we hypothesize that the loss of *Crip2* similarly affects the migration and adhesion of notochord cells. This dysfunction could consequently lead to the abnormal nuclear aggregation observed in the notochord.

PDE10A, a member of the PDE10 protein family, catalyzes the hydrolysis of both cAMP and cGMP, affecting various cellular functions such as vascular tone and vascular cell proliferation [73]. RNA-seq analysis revealed that PDE10A/cAMP signaling is disrupted in *CRIP2* mutant cells. Inhibition of PDE10A enhances cell death, decreases proliferation, and sensitizes human cancer cells to doxorubicin [104]. PKA and PKG, key effectors of cAMP and cGMP, respectively, are implicated in cell growth. PKG has two splicing isoforms, PKG1 α and PKG1 β , which have opposing effects on SMC proliferation in vitro: PKG1 α inhibits SMC proliferation, whereas PKG1 β promotes SMC proliferation [73]. Both PKA and exchange protein activated by cAMP (EPAC) collaborate to inhibit VSMC proliferation via actin cytoskeleton remodeling and the modulation of SRF and TEAD, which regulate the expression of genes required

for proliferation [74]. Our qRT-PCR results revealed a significant decrease in *PKG1 β* , *PRKACA* and *PRKACB* (PKA family members), indicating that CRIP2 regulates cell proliferation, at least in part, through these pathways.

Furthermore, F2R (also known as PAR1), which promotes cortical actin caps and influences actin cytoskeletal organization [105], was significantly upregulated upon CRIP2 loss. This regulation may contribute to the increase in KRT8 and VIM, providing a partial explanation for the altered cytoskeletal dynamics observed in CRIP2-deficient cells. PDGF/PDGFR signaling is integral to cell proliferation, metastasis, invasion, angiogenesis, and modulates multiple downstream pathways. The activation of the JAK-STAT pathway can result in the transcription of vital genes [106]; PDGFB activates the JAK/STAT1/3 pathway via PDGFRB to promote mitotic signals [16], and PDGF signaling drives proliferation through SRF at the midface [75, 107]. Our research revealed that CRIP2 loss diminished PDGF/JAK/STAT signaling and demonstrated that CRIP2 could bind to SRF, which led to altered expression of cell cycle regulators, with a significant increase in p21 and a decrease in CDK1, CDK2 and CCND2, which are pivotal for cell cycle progression. In line with these findings, CDKs are pivotal for cell cycle progression [108]. PDGF signaling is known to drive proliferation via SRF, with a subset of SRF target genes involved in focal adhesion and cytoskeletal organization crucial for cell migration [75]. It is of interest to explore whether the CRIP2/SRF interaction directly regulates cytoskeleton proteins, including intermediate filament proteins such as KRT8 and VIM, which could have implications for cell migration and structure.

Overall, we elucidated a novel mechanism in which CRIP2 is crucial for vascular development by interacting with SRF, KRT8 and VIM. This interaction not only regulates the function of CRIP2 but also modulates downstream factors, thereby controlling the migration, adhesion and proliferation of endothelial cells. This research provides novel insights into the role of CRIP2 in mediating cell behavior and proliferation during cardiovascular development, and exploring the potential applications of these findings in cardiovascular disorders is particularly intriguing.

Supplementary Information The online version contains supplementary material available at <https://doi.org/10.1007/s00018-025-05624-w>.

Acknowledgements The authors would like to thank Prof. LI Jing (School of Medicine and Pharmacy, Ocean University of China) for sharing the HUVECs and Prof. ZHAO Chengtian (College of Marine Life Sciences, Ocean University of China) for sharing the plasmids.

Author contributions All the authors have read and agreed to the published version of the manuscript. H.L. and S.Y. designed the research, and S.Y. performed the experiments. S.Y., X.Z., and X.L. analyzed the data and prepared the figures. S.Y. and H.L. prepared the figures and

wrote the manuscript.

Funding This work was supported by grants from the Natural Science Foundation of China [32171139, 32471162, 31872187], the Science & Technology Innovation Project of Laoshan Laboratory (LSKJ202203204) and the Qingdao Postdoctoral Science Foundation (QDBSH20240102157).

Data availability The original contributions presented in this study are included in the article/Supplementary Materials. Further inquiries can be directed to the corresponding author.

Declarations

Institutional review board statement The study was approved by the Ocean University of China Institutional Animal Care and Use Committee (OUC-AE-2021-234) prior to the initiation of the study. All experiments and relevant methods were carried out in accordance with the approved guidelines and regulations of OUC-IACUC.

Competing interests The authors declare that the research was conducted in the absence of any commercial or financial relationships that could be construed as potential conflicts of interest.

Open Access This article is licensed under a Creative Commons Attribution-NonCommercial-NoDerivatives 4.0 International License, which permits any non-commercial use, sharing, distribution and reproduction in any medium or format, as long as you give appropriate credit to the original author(s) and the source, provide a link to the Creative Commons licence, and indicate if you modified the licensed material. You do not have permission under this licence to share adapted material derived from this article or parts of it. The images or other third party material in this article are included in the article's Creative Commons licence, unless indicated otherwise in a credit line to the material. If material is not included in the article's Creative Commons licence and your intended use is not permitted by statutory regulation or exceeds the permitted use, you will need to obtain permission directly from the copyright holder. To view a copy of this licence, visit <http://creativecommons.org/licenses/by-nc-nd/4.0/>.

References

- Toth G, Cerejo R (2018) Intracranial aneurysms: review of current science and management. *Vasc Med* 23:276–288. <https://doi.org/10.1177/1358863X18754693>
- Polubothu S (2021) Genotype-guided medical treatment of arteriovenous malformation. *Clin Exp Dermatol* 46:800–801. <https://doi.org/10.1111/ced.14439>
- Hage AN, Chick JFB, Srinivasa RN, Bundy JJ, Chauhan NR, Acord M, Gemmete JJ (2018) Treatment of venous malformations: the data, where we are, and how it is done. *Tech Vasc Interv Radiol* 21:45–54
- Ma S, Duan S, Liu Y, Wang H (2022) Intimal hyperplasia of arteriovenous fistula. *Ann Vasc Surg* 85:444–453. <https://doi.org/10.1016/j.avsg.2022.04.030>
- Gross BA, Jankowitz BT, Friedlander RM (2019) Cerebral intraparenchymal hemorrhage: A review. *JAMA* 321:1295–1303. <https://doi.org/10.1001/jama.2019.2413>
- Ehresman J, Catapano JS, Baranoski JF, Jadhav AP, Ducruet AF, Albuquerque FC (2022) Treatment of spinal arteriovenous malformation and fistula. *Neurosurg Clin N Am* 33:193–206. <https://doi.org/10.1016/j.nec.2021.11.005>
- Kassmeyer S, Plendl J, Custodis P, Bahramsoltani M (2009) New insights in vascular development: vasculogenesis and endothelial progenitor cells. *Anat Histol Embryol* 38:1–11. <https://doi.org/10.1111/j.1439-0264.2008.00894.x>
- Viallard C, Larrivee B (2017) Tumor angiogenesis and vascular normalization: alternative therapeutic targets. *Angiogenesis* 20:409–426. <https://doi.org/10.1007/s10456-017-9562-9>
- Jin SW, Patterson C (2009) The opening act: vasculogenesis and the origins of circulation. *Arterioscler Thromb Vasc Biol* 29:623–629. <https://doi.org/10.1161/ATVBAHA.107.161539>
- Porcher C, Chagraoui H, Kristiansen MS (2017) SCL/TAL1: a multifaceted regulator from blood development to disease. *Blood* 129:2051–2060. <https://doi.org/10.1182/blood-2016-12-754051>
- Ishige-Wada M, Kwon SM, Eguchi M, Hozumi K, Iwaguro H, Matsumoto T, Fukuda N, Mugishima H, Masuda H, Asahara T (2016) Jagged-1 signaling in the bone marrow microenvironment promotes endothelial progenitor cell expansion and commitment of CD133+ Human cord blood cells for postnatal vasculogenesis. *PLoS ONE* 11:e0166660. <https://doi.org/10.1371/journal.pone.0166660>
- Roskoski R Jr. (2017) Vascular endothelial growth factor (VEGF) and VEGF receptor inhibitors in the treatment of renal cell carcinomas. *Pharmacol Res* 120:116–132. <https://doi.org/10.1016/j.phrs.2017.03.010>
- Benedito R, Roca C, Sorensen I, Adams S, Gossler A, Fruttiger M, Adams RH (2009) The Notch ligands Dll4 and Jagged1 have opposing effects on angiogenesis. *Cell* 137:1124–1135. <https://doi.org/10.1016/j.cell.2009.03.025>
- Riahi R, Sun J, Wang S, Long M, Zhang DD, Wong PK (2015) Notch1-Dll4 signalling and mechanical force regulate leader cell formation during collective cell migration. *Nat Commun* 6:6556. <https://doi.org/10.1038/ncomms7556>
- Apte RS, Chen DS, Ferrara N (2019) VEGF in signaling and disease: beyond discovery and development. *Cell* 176:1248–1264. <https://doi.org/10.1016/j.cell.2019.01.021>
- Zou X, Tang XY, Qu ZY, Sun ZW, Ji CF, Li YJ, Guo SD (2022) Targeting the PDGF/PDGFR signaling pathway for cancer therapy: A review. *Int J Biol Macromol* 202:539–557. <https://doi.org/10.1016/j.ijbiomac.2022.01.113>
- Saia L, Gomes A, Cazales M, Ducommun B, Lobjois V (2015) Cell-Cell adhesion and cytoskeleton tension oppose each other in regulating tumor cell aggregation. *Cancer Res* 75:2426–2433. <https://doi.org/10.1158/0008-5472.CAN-14-3534>
- Li G, Satyamoorthy K, Herlyn M (2001) N-cadherin-mediated intercellular interactions promote survival and migration of melanoma cells. *Cancer Res* 61:3819–3825
- Young TH, Tu HR, Chan CC, Huang YC, Yen MH, Cheng NC, Chiu HC, Lin SJ (2009) The enhancement of dermal papilla cell aggregation by extracellular matrix proteins through effects on cell-substratum adhesivity and cell motility. *Biomaterials* 30:5031–5040. <https://doi.org/10.1016/j.biomaterials.2009.05.065>
- Geng Y, Chandrasekaran S, Hsu JW, Gidwani M, Hughes AD, King MR (2013) Phenotypic switch in blood: effects of pro-inflammatory cytokines on breast cancer cell aggregation and adhesion. *PLoS ONE* 8:e54959. <https://doi.org/10.1371/journal.pone.0054959>
- Mui KL, Chen CS, Assoian RK (2016) The mechanical regulation of integrin-cadherin crosstalk organizes cells, signaling and forces. *J Cell Sci* 129:1093–1100. <https://doi.org/10.1242/jcs.183699>
- Tixi W, Maldonado M, Chang YT, Chiu A, Yeung W, Parveen N, Nelson MS, Hart R, Wang S, Hsu WJ, Fueger P, Kopp JL, Huising MO, Dhawan S, Shih HP (2023) Coordination between ECM and cell-cell adhesion regulates the development of islet

- aggregation, architecture, and functional maturation. *Elife* 12. <https://doi.org/10.7554/eLife.90006>
23. Canel M, Serrels A, Frame MC, Brunton VG (2013) E-cadherin-integrin crosstalk in cancer invasion and metastasis. *J Cell Sci* 126:393–401. <https://doi.org/10.1242/jcs.100115>
 24. van Roy F, Berx G (2008) The cell-cell adhesion molecule E-cadherin. *Cell Mol Life Sci* 65:3756–3788. <https://doi.org/10.1007/s00018-008-8281-1>
 25. Pollard TD, Goldman RD (2018) Overview of the cytoskeleton from an evolutionary perspective. *Cold Spring Harb Perspect Biol* 10. <https://doi.org/10.1101/cshperspect.a030288>
 26. Gould NR, Torre OM, Leser JM, Stains JP (2021) The cytoskeleton and connected elements in bone cell mechano-transduction. *Bone* 149:115971. <https://doi.org/10.1016/j.bone.2021.115971>
 27. Bays JL, DeMali KA (2017) Vinculin in cell-cell and cell-matrix adhesions. *Cell Mol Life Sci* 74:2999–3009. <https://doi.org/10.1007/s00018-017-2511-3>
 28. Etienne-Manneville S (2018) Cytoplasmic intermediate filaments in cell biology. *Annu Rev Cell Dev Biol* 34:1–28. <https://doi.org/10.1146/annurev-cellbio-100617-062534>
 29. Ohi R, Zanic M (2016) Ahead of the curve: new insights into microtubule dynamics. *F1000Res* 5. <https://doi.org/10.12688/f1000research.7439.1>
 30. Hohmann T, Dehghani F (2019) The cytoskeleton—a complex interacting meshwork. *Cells* 8. <https://doi.org/10.3390/cells8040362>
 31. Herrmann H, Aebi U (2004) Intermediate filaments: molecular structure, assembly mechanism, and integration into functionally distinct intracellular scaffolds. *Annu Rev Biochem* 73:749–789. <https://doi.org/10.1146/annurev.biochem.73.011303.073823>
 32. Kadrmas JL, Beckerle MC (2004) The LIM domain: from the cytoskeleton to the nucleus. *Nat Rev Mol Cell Biol* 5:920–931. <https://doi.org/10.1038/nrm1499>
 33. Matthews JM, Lester K, Joseph S, Curtis DJ (2013) LIM-domain-only proteins in cancer. *Nat Rev Cancer* 13:111–122. <https://doi.org/10.1038/nrc3418>
 34. Razzell W, Bustillo ME, Zallen JA (2018) The force-sensitive protein Ajuba regulates cell adhesion during epithelial morphogenesis. *J Cell Biol* 217:3715–3730. <https://doi.org/10.1083/jcb.201801171>
 35. Zhong C, Li X, Tao B, Peng L, Peng T, Yang X, Xia X, Chen L (2019) LIM and SH3 protein 1 induces glioma growth and invasion through PI3K/AKT signaling and epithelial-mesenchymal transition. *Biomed Pharmacother* 116:109013. <https://doi.org/10.1016/j.biopha.2019.109013>
 36. Jiang CY, Yu JJ, Ruan Y, Wang XH, Zhao W, Wang XJ, Zhu YP, Gao Y, Hao KY, Chen L, Han BM, Xia SJ, Zhao FJ (2016) LIM domain only 2 over-expression in prostate stromal cells facilitates prostate cancer progression through paracrine of Interleukin-11. *Oncotarget* 7:26247–26258. <https://doi.org/10.18632/oncotarget.8359>
 37. Anderson CA, Kovar DR, Gardel ML, Winkelman JD (2021) LIM domain proteins in cell mechanobiology. *Cytoskeleton (Hoboken)* 78:303–311. <https://doi.org/10.1002/cm.21677>
 38. Smith MA, Hoffman LM, Beckerle MC (2014) LIM proteins in actin cytoskeleton mechanoresponse. *Trends Cell Biol* 24:575–583. <https://doi.org/10.1016/j.tcb.2014.04.009>
 39. Freyd G, Kim SK, Horvitz HR (1990) Novel cysteine-rich motif and homeodomain in the product of the *Caenorhabditis elegans* cell lineage gene *lin-11*. *Nature* 344:876–879. <https://doi.org/10.1038/344876a0>
 40. Schiller HB, Friedel CC, Boulegue C, Fassler R (2011) Quantitative proteomics of the integrin adhesome show a myosin II-dependent recruitment of LIM domain proteins. *EMBO Rep* 12:259–266. <https://doi.org/10.1038/embor.2011.5>
 41. Zhang LZ, Huang LY, Huang AL, Liu JX, Yang F (2018) CRIP1 promotes cell migration, invasion and epithelial-mesenchymal transition of cervical cancer by activating the Wnt/beta-catenin signaling pathway. *Life Sci* 207:420–427. <https://doi.org/10.1016/j.lfs.2018.05.054>
 42. He G, Zou L, Zhou L, Gao P, Qian X, Cui J (2017) Cysteine-Rich intestinal protein 1 Silencing inhibits migration and invasion in human colorectal Cancer. *Cell Physiol Biochem* 44:897–906. <https://doi.org/10.1159/000485357>
 43. Ludyga N, Englert S, Pflieger K, Rauser S, Braselmann H, Walch A, Auer G, Hofler H, Aubele M (2013) The impact of cysteine-rich intestinal protein 1 (CRIP1) in human breast cancer. *Mol Cancer* 12:28. <https://doi.org/10.1186/1476-4598-12-28>
 44. Kim JD, Kim HJ, Koun S, Ham HJ, Kim MJ, Rhee M, Huh TL (2014) Zebrafish Crip2 plays a critical role in atrioventricular valve development by downregulating the expression of ECM genes in the endocardial cushion. *Mol Cells* 37:406–411. <https://doi.org/10.14348/molcells.2014.0072>
 45. Sun X, Zhang R, Lin X, Xu X (2008) Wnt3a regulates the development of cardiac neural crest cells by modulating expression of cysteine-rich intestinal protein 2 in rhombomere 6. *Circ Res* 102:831–839. <https://doi.org/10.1161/CIRCRESAHA.107.166488>
 46. Wei TC, Lin HY, Lu CC, Chen CM, You LR (2011) Expression of Crip2, a LIM-domain-only protein, in the mouse cardiovascular system under physiological and pathological conditions. *Gene Expr Patterns* 11:384–394. <https://doi.org/10.1016/j.gexp.2011.05.001>
 47. Kwan KM, Fujimoto E, Grabher C, Mangum BD, Hardy ME, Campbell DS, Parant JM, Yost HJ, Kanki JP, Chien CB (2007) The Tol2kit: a multisite gateway-based construction kit for Tol2 transposon transgenesis constructs. *Dev Dyn* 236:3088–3099. <https://doi.org/10.1002/dvdy.21343>
 48. Kimmel CB, Ballard WW, Kimmel SR, Ullmann B, Schilling TF (1995) Stages of embryonic development of the zebrafish. *Dev Dyn* 203:253–310. <https://doi.org/10.1002/aja.1002030302>
 49. Thisse TC B (2008) High-resolution in situ hybridization to whole-mount zebrafish embryos. *Nat Protoc* 3:59–69. <https://doi.org/10.1038/nprot.2007.514>
 50. Yang S, Zhang X, Li X, Yin X, Teng L, Ji G, Li H (2022) Evolutionary and expression analysis of MOV10 and MOV10L1 reveals their origin, duplication and divergence. *Int J Mol Sci* 23. <https://doi.org/10.3390/ijms23147523>
 51. Yang S, Xu X, Zhang A, Wang Y, Ji G, Sun C, Li H (2023) The evolution and Immunomodulatory role of Zc3h12 proteins in zebrafish (*Danio rerio*). *Int J Biol Macromol* 239:124214. <https://doi.org/10.1016/j.ijbiomac.2023.124214>
 52. Lin A, Giuliano CJ, Sayles NM, Sheltzer JM (2017) CRISPR/Cas9 mutagenesis invalidates a putative cancer dependency targeted in on-going clinical trials. *Elife* 6. <https://doi.org/10.7554/eLife.24179>
 53. Gu X, Han S, Cui M, Xue J, Ai L, Sun L, Zhu X, Wang Y, Liu C (2019) Knockdown of endothelin receptor B inhibits the progression of triple-negative breast cancer. *Ann N Y Acad Sci* 1448:5–18. <https://doi.org/10.1111/nyas.14039>
 54. Wang P, Zhang X, Zheng X, Gao J, Shang M, Xu J, Liang H (2022) Folic acid protects against hyperuricemia in C57BL/6J mice via ameliorating Gut-Kidney Axis dysfunction. *J Agric Food Chem* 70:15787–15803. <https://doi.org/10.1021/acs.jafc.2c06297>
 55. Gering M, Rodaway AR, Gottgens B, Patient RK, Green AR (1998) The SCL gene specifies haemangioblast development from early mesoderm. *EMBO J* 17:4029–4045. <https://doi.org/10.1093/emboj/17.14.4029>
 56. Dooley KA, Davidson AJ, Zon LI (2005) Zebrafish Scl functions independently in hematopoietic and endothelial development.

- Dev Biol 277:522–536. <https://doi.org/10.1016/j.ydbio.2004.09.004>
57. Patterson LJ, Gering M, Patient R (2005) Sc1 is required for dorsal aorta as well as blood formation in zebrafish embryos. *Blood* 105:3502–3511. <https://doi.org/10.1182/blood-2004-09-3547>
 58. Cao X, Li T, Xu B, Ding K, Li W, Shen B, Chu M, Zhu D, Rui L, Shang Z, Li X, Wang Y, Zheng S, Alitalo K, Liu G, Tang J, Kubota Y, He Y (2023) Endothelial TIE1 restricts angiogenic sprouting to coordinate vein assembly in synergy with its homologue TIE2. *Arterioscler Thromb Vasc Biol* 43:e323–e338. <https://doi.org/10.1161/ATVBAHA.122.318860>
 59. Brown LA, Rodaway AR, Schilling TF, Jowett T, Ingham PW, Patient RK, Sharrocks AD (2000) Insights into early vasculogenesis revealed by expression of the ETS-domain transcription factor Fli-1 in wild-type and mutant zebrafish embryos. *Mech Dev* 90:237–252. [https://doi.org/10.1016/s0925-4773\(99\)00256-7](https://doi.org/10.1016/s0925-4773(99)00256-7)
 60. Tang X, Wu H, Xie J, Wang N, Chen Q, Zhong Z, Qiu Y, Wang J, Li X, Situ P, Lai L, Zern MA, Chen H, Duan Y (2021) The combination of dextran sulphate and Polyvinyl alcohol prevents excess aggregation and promotes proliferation of pluripotent stem cells in suspension culture. *Cell Prolif* 54:e13112. <https://doi.org/10.1111/cpr.13112>
 61. Andl CD, Mizushima T, Nakagawa H, Oyama K, Harada H, Churma K, Herlyn M, Rustgi AK (2003) Epidermal growth factor receptor mediates increased cell proliferation, migration, and aggregation in esophageal keratinocytes in vitro and in vivo. *J Biol Chem* 278:1824–1830. <https://doi.org/10.1074/jbc.M209148200>
 62. Kwon TG, Yang TD, Lee KJ (2016) Enhancement of chemotactic cell aggregation by Haptotactic cell-To-Cell interaction. *PLoS ONE* 11:e0154717. <https://doi.org/10.1371/journal.pone.0154717>
 63. Pope MD, Asthagiri AR (2012) Short-lived, transitory cell-cell interactions foster migration-dependent aggregation. *PLoS ONE* 7:e43237. <https://doi.org/10.1371/journal.pone.0043237>
 64. Beutel O, Maraschini R, Pombo-Garcia K, Martin-Lemaitre C, Honigsmann A (2019) Phase separation of Zonula occludens proteins drives formation of tight junctions. *Cell* 179:923–936e911. <https://doi.org/10.1016/j.cell.2019.10.011>
 65. Zhao ZQ Y (2007) The diverse biofunctions of LIM domain proteins: determined by subcellular localization and protein-protein interaction. *Biol Cell* 99:489–502. <https://doi.org/10.1042/BC20060126>
 66. Chen H, Chen X, Pan B, Zheng C, Hong L, Han W (2022) KRT8 serves as a novel biomarker for LUAD and promotes metastasis and EMT via NF-kappaB signaling. *Front Oncol* 12:875146. <https://doi.org/10.3389/fonc.2022.875146>
 67. Jacob JT, Coulombe PA, Kwan R, Omary MB (2018) Types I and II keratin intermediate filaments. *Cold Spring Harb Perspect Biol* 10. <https://doi.org/10.1101/cshperspect.a018275>
 68. Kuburich NA, den Hollander P, Pietz JT, Mani SA (2022) Vimentin and cytokeratin: good alone, bad together. *Semin Cancer Biol* 86:816–826. <https://doi.org/10.1016/j.semcancer.2021.12.006>
 69. Salhia B, Kiefer J, Ross JT, Metapally R, Martinez RA, Johnson KN, DiPerna DM, Paquette KM, Jung S, Nasser S, Wallstrom G, Tembe W, Baker A, Carpten J, Resau J, Ryken T, Sibenaller Z, Petricoin EF, Liotta LA, Ramanathan RK, Berens ME, Tran NL (2014) Integrated genomic and epigenomic analysis of breast cancer brain metastasis. *PLoS ONE* 9:e85448. <https://doi.org/10.1371/journal.pone.0085448>
 70. Fang J, Wang H, Liu Y, Ding F, Ni Y, Shao S (2017) High KRT8 expression promotes tumor progression and metastasis of gastric cancer. *Cancer Sci* 108:178–186. <https://doi.org/10.1111/cas.13120>
 71. Shao W, Li J, Piao Q, Yao X, Li M, Wang S, Song Z, Sun Y, Zheng L, Wang G, Liu L, Yu C, Huang Y, Bao Y, Sun L (2023) FRMD3 inhibits the growth and metastasis of breast cancer through the ubiquitination-mediated degradation of vimentin and subsequent impairment of focal adhesion. *Cell Death Dis* 14:13. <https://doi.org/10.1038/s41419-023-05552-2>
 72. Geng A, Luo L, Ren F, Zhang L, Zhou H, Gao X (2021) miR-29a-3p inhibits endometrial cancer cell proliferation, migration and invasion by targeting VEGFA/CD C42/PAK1. *BMC Cancer* 21:843. <https://doi.org/10.1186/s12885-021-08506-z>
 73. Luo L, Cai Y, Zhang Y, Hsu CG, Korshunov VA, Long X, Knight PA, Berk BC, Yan C (2022) Role of PDE10A in vascular smooth muscle cell hyperplasia and pathological vascular remodelling. *Cardiovasc Res* 118:2703–2717. <https://doi.org/10.1093/cvr/cva6304>
 74. Smith SA, Newby AC, Bond M (2019) Ending restenosis: inhibition of vascular smooth muscle cell proliferation by cAMP. *Cells* 8. <https://doi.org/10.3390/cells8111447>
 75. Vasudevan HN, Soriano P (2014) SRF regulates craniofacial development through selective recruitment of MRTF cofactors by PDGF signaling. *Dev Cell* 31:332–344. <https://doi.org/10.1016/j.devcel.2014.10.005>
 76. Chen Y, Surinkaew S, Naud P, Qi XY, Gillis MA, Shi YF, Tardif JC, Dobrev D, Nattel S (2017) JAK-STAT signalling and the atrial fibrillation promoting fibrotic substrate. *Cardiovasc Res* 113:310–320. <https://doi.org/10.1093/cvr/cvx004>
 77. Zhu H, Zheng C (2021) When PARPs Meet antiviral innate immunity. *Trends Microbiol* 29:776–778. <https://doi.org/10.1016/j.tim.2021.01.002>
 78. Zhou L, Wang Y, Zhou M, Zhang Y, Wang P, Li X, Yang J, Wang H, Ding Z (2018) HOXA9 inhibits HIF-1alpha-mediated Glycolysis through interacting with CRIP2 to repress cutaneous squamous cell carcinoma development. *Nat Commun* 9:1480. <https://doi.org/10.1038/s41467-018-03914-5>
 79. Lo PH, Ko JM, Yu ZY, Law S, Wang LD, Li JL, Srivastava G, Tsao SW, Stanbridge EJ, Lung ML (2012) The LIM domain protein, CRIP2, promotes apoptosis in esophageal squamous cell carcinoma. *Cancer Lett* 316:39–45. <https://doi.org/10.1016/j.canl.2011.10.020>
 80. Li F, Bing Z, Chen W, Ye F, Liu Y, Ding L, Jin X (2021) Prognosis biomarker and potential therapeutic target CRIP2 associated with radiosensitivity in NSCLC cells. *Biochem Biophys Res Commun* 584:73–79. <https://doi.org/10.1016/j.bbrc.2021.11.002>
 81. Xie Y, Ostriker AC, Jin Y, Hu H, Sizer AJ, Peng G, Morris AH, Ryu C, Herzog EL, Kyriakides T, Zhao H, Dardik A, Yu J, Hwa J, Martin KA (2019) LMO7 is a negative feedback regulator of transforming growth factor beta signaling and fibrosis. *Circulation* 139:679–693. <https://doi.org/10.1161/CIRCULATIONAHA.118.034615>
 82. Yamada Y, Pannell R, Forster A, Rabbitts TH (2000) The oncogenic LIM-only transcription factor Lmo2 regulates angiogenesis but not vasculogenesis in mice. *Proc Natl Acad Sci U S A* 97:320–324. <https://doi.org/10.1073/pnas.97.1.320>
 83. Kurakula K, Vos M, Otermin Rubio I, Marinkovic G, Buettner R, Heukamp LC, Stap J, de Waard V, van Tiel CM, de Vries CJ (2014) The LIM-only protein FHL2 reduces vascular lesion formation involving Inhibition of proliferation and migration of smooth muscle cells. *PLoS ONE* 9:e94931. <https://doi.org/10.1371/journal.pone.0094931>
 84. Wang F, Zhao J, Zhang M, Yang J, Zeng G (2021) Genome-wide analysis of the mouse LIM gene family reveals its roles in regulating pathological cardiac hypertrophy. *FEBS Lett* 595:2271–2289. <https://doi.org/10.1002/1873-3468.14168>
 85. Hempel A, Kuhl SJ (2014) Comparative expression analysis of cysteine-rich intestinal protein family members cripl, 2 and 3 during *Xenopus laevis* embryogenesis. *Int J Dev Biol* 58:841–849. <https://doi.org/10.1387/ijdb.140270sk>

86. Cheung AK, Ko JM, Lung HL, Chan KW, Stanbridge EJ, Zabarovsky E, Tokino T, Kashima L, Suzuki T, Kwong DL, Chua D, Tsao SW, Lung ML (2011) Cysteine-rich intestinal protein 2 (CRIP2) acts as a repressor of NF-kappaB-mediated proangiogenic cytokine transcription to suppress tumorigenesis and angiogenesis. *Proc Natl Acad Sci U S A* 108:8390–8395. <https://doi.org/10.1073/pnas.1101747108>
87. Shi W, Bruce J, Lee M, Yue S, Rowe M, Pintilie M, Kogo R, Bissey PA, Fyles A, Yip KW, Liu FF (2016) MiR-449a promotes breast cancer progression by targeting CRIP2. *Oncotarget* 7:18906–18918. <https://doi.org/10.18632/oncotarget.7753>
88. Gao X, Sun JY, Cao ZY, Lin Y, Zha DJ, Wang F, Xue T, Qiao L, Lu LJ, Qiu JH (2009) Polyclonal antibodies to LIM proteins CRP2 and CRIP2 reveal their subcellular localizations in olfactory precursor cells. *Biochem (Mosc)* 74:336–341. <https://doi.org/10.1134/s0006297909030134>
89. Kihara T, Sugimoto Y, Shinohara S, Takaoka S, Miyake J (2017) Cysteine-rich protein 2 accelerates actin filament cluster formation. *PLoS ONE* 12:e0183085. <https://doi.org/10.1371/journal.pone.0183085>
90. Noetzel E, Rose M, Sevinc E, Hilgers RD, Hartmann A, Naami A, Knuchel R, Dahl E (2010) Intermediate filament dynamics and breast cancer: aberrant promoter methylation of the Synemin gene is associated with early tumor relapse. *Oncogene* 29:4814–4825. <https://doi.org/10.1038/ncr.2010.229>
91. Kim DS, Cheah JS, Lai TW, Zhao KX, Foust SR, Julie Lee YR, Lo SH, Heinrich V, Yamada S (2024) Tandem LIM domain-containing proteins, LIMK1 and LMO1, directly bind to force-bearing keratin intermediate filaments. *Cell Rep* 43:114480. <https://doi.org/10.1016/j.celrep.2024.114480>
92. Zienert E, Eke I, Aust D, Cordes N (2015) LIM-only protein FHL2 critically determines survival and radioresistance of pancreatic cancer cells. *Cancer Lett* 364:17–24. <https://doi.org/10.1016/j.canlet.2015.04.019>
93. Hoang MV, Nagy JA, Senger DR (2011) Cdc42-mediated Inhibition of GSK-3beta improves angio-architecture and lumen formation during VEGF-driven pathological angiogenesis. *Microvasc Res* 81:34–43. <https://doi.org/10.1016/j.mvr.2010.09.001>
94. Huang D, Qiu H, Miao L, Guo L, Zhang X, Lin M, Li Z, Li F (2022) Cdc42 promotes thyroid cancer cell proliferation and migration and tumor-associated macrophage polarization through the PTEN/AKT pathway. *J Biochem Mol Toxicol* 36:e23115. <https://doi.org/10.1002/jbt.23115>
95. Ma LL, Guo LL, Luo Y, Liu GL, Lei Y, Jing FY, Zhang YL, Tong GH, Jing ZL, Shen L, Tang MS, Ding YQ, Deng YJ (2020) Cdc42 subcellular relocation in response to VEGF/NRP1 engagement is associated with the poor prognosis of colorectal cancer. *Cell Death Dis* 11:171. <https://doi.org/10.1038/s41419-020-2370-y>
96. Ke J, Wu G, Zhang J, Li H, Gao S, Shao M, Gao Z, Sy MS, Cao Y, Yang X, Xu J, Li C (2020) Melanoma migration is promoted by prion protein via Akt-hsp27 signaling axis. *Biochem Biophys Res Commun* 523:375–381. <https://doi.org/10.1016/j.bbrc.2019.12.042>
97. Zhang C, Cheng H, Ye X, Cui H, Li Y, Zhu H, Chang X (2024) ECM1 promotes migration and invasion in endometriosis. *Reprod Biol* 24:100826. <https://doi.org/10.1016/j.repbio.2023.100826>
98. Gomes ER, Jani S, Gundersen GG (2005) Nuclear movement regulated by Cdc42, MRCK, myosin, and actin flow establishes MTOC polarization in migrating cells. *Cell* 121:451–463. <https://doi.org/10.1016/j.cell.2005.02.022>
99. van Hinsbergh VW, Engelse MA, Quax PH (2006) Pericellular proteases in angiogenesis and vasculogenesis. *Arterioscler Thromb Vasc Biol* 26:716–728. <https://doi.org/10.1161/01.ATV.0000209518.58252.17>
100. Wu Q, Sun S, Wei L, Liu M, Liu H, Liu T, Zhou Y, Jia Q, Wang D, Yang Z, Duan M, Yang X, Gao P, Ning X (2022) Twist1 regulates macrophage plasticity to promote renal fibrosis through galectin-3. *Cell Mol Life Sci* 79:137. <https://doi.org/10.1007/s00018-022-04137-0>
101. Balmer S, Nowotschin S, Hadjantonakis AK (2016) Notochord morphogenesis in mice: current Understanding & open questions. *Dev Dyn* 245:547–557. <https://doi.org/10.1002/dvdy.24392>
102. Jiang D, Munro EM, Smith WC (2005) Ascidian prickle regulates both mediolateral and anterior-posterior cell Polarity of notochord cells. *Curr Biol* 15:79–85. <https://doi.org/10.1016/j.cub.2004.12.041>
103. Peng H, Qiao R, Dong B (2020) Polarity establishment and maintenance in Ascidian notochord. *Front Cell Dev Biol* 8:597446. <https://doi.org/10.3389/fcell.2020.597446>
104. Chen S, Chen J, Du W, Mickelsen DM, Shi H, Yu H, Kumar S, Yan C (2023) PDE10A inactivation prevents Doxorubicin-Induced cardiotoxicity and tumor growth. *Circ Res* 133:138–157. <https://doi.org/10.1161/CIRCRESAHA.122.322264>
105. Jiang T, Harris TJC (2019) Par-1 controls the composition and growth of cortical actin caps during Drosophila embryo cleavage. *J Cell Biol* 218:4195–4214. <https://doi.org/10.1083/jcb.201903152>
106. Yuan H, You J, You H, Zheng C (2018) Herpes simplex virus 1 UL36USP antagonizes type I Interferon-Mediated antiviral innate immunity. *J Virol* 92. <https://doi.org/10.1128/JVI.01161-18>
107. Rana N, Privitera G, Kondolf HC, Bulek K, Lechuga S, De Salvo C, Corridoni D, Antanaviciute A, Maywald RL, Hurtado AM, Zhao J, Huang EH, Li X, Chan ER, Simmons A, Bamias G, Abbott DW, Heaney JD, Ivanov AI, Pizarro TT (2022) GSDMB is increased in IBD and regulates epithelial restitution/repair independent of pyroptosis. *Cell* 185:283–298e217. <https://doi.org/10.1016/j.cell.2021.12.024>
108. Zheng C, Tang YD (2022) The emerging roles of the CDK/cyclin complexes in antiviral innate immunity. *J Med Virol* 94:2384–2387. <https://doi.org/10.1002/jmv.27554>

Publisher's note Springer Nature remains neutral with regard to jurisdictional claims in published maps and institutional affiliations.